1
Nanotechnology and Tissue Engineering: The Scaffold Based Approach

Lakshmi S. Nair, Subhabrata Bhattacharyya, and Cato T. Laurencin

1.1
Overview

Biodegradable porous three-dimensional (3D) structures have been extensively used as scaffolds for tissue engineering to temporarily mimic the structure and functions of the natural extracellular matrix (ECM). The ECM functions to provide 3D structure with mechanical and biochemical cues to support and control cell organization and functions. Even though macro- and micro-fabrication techniques enabled the development of highly porous 3D scaffolds that could support the adhesion and proliferation of cells, their ability to closely mimic the complex nanostructured topography and biochemical functions of the ECM is far from optimal. However, recent developments in nanofabrication techniques have afforded various nanostructured bioactive scaffolds. These include top-down approaches such as electrospinning and phase separation to develop nanofibrous scaffolds from polymer solutions or bottom-up approaches such as self-assembly to develop nanofibrous scaffolds from specifically designed bioactive peptide motifs. Although significant improvements are needed for these nanofabrication processes to produce scaffolds that could precisely mimic the structure and functions of the ECM, the developments so far have significantly enhanced our ability to recreate the natural cellular environment for regenerating tissues.

1.2
Introduction

Tissue engineering has now emerged from the stage of infancy demonstrating proof of principle and developing various functional tissues using different approaches to the stage of an established scientific discipline capable of developing viable products for clinical applications. Tissue engineered skin can be considered as one of the first commercialized products developed using the principles of tissue engineering. In addition to clinical applications, tissue engineering has also

Nanotechnologies for the Life Sciences Vol. 9
Tissue, Cell and Organ Engineering. Edited by Challa S. S. R. Kumar

ISBN: 3-527-31389-3

raised significant interest as a novel tool for investigating cell and developmental biology and developing novel drugs using tissues grown in 3D environments [1].

The ultimate goal of tissue engineering is to address the current organ shortage problem, i.e., development of an alternative therapeutic strategy to autografting and allografting, two common approaches currently used to repair or reconstruct damaged tissues or organs. Autografts and allografts have several shortcomings that significantly limit their applications. These include limited availability and donor site morbidity associated with autografts and risk of infection and immunogenicity associated with allografts [2]. Conversely, regeneration or repair of tissue using tissue engineering approaches attempts to recreate functional tissue using bioresorbable synthetic materials and other required components that can be routinely assembled and reliably integrated into the body without any of the abovementioned adverse side effects. Tissue engineering thus holds promise to revolutionize current health care approaches to improve the quality of human life in a practical and affordable way.

The term ''tissue engineering'' was coined in 1987 during a National Science Foundation (NSF) Meeting inspired by a concept presented by Dr. Y.C. Fung of the University of California at San Diego [3]. At a subsequent workshop held by NSF in 1988, tissue engineering was defined as ''the application of principles and methods of engineering and life sciences to obtain a fundamental understanding of structure–function relationships in novel and pathological mammalian tissues and the development of biological substitutes to restore, maintain and improve tissue functions'' [4]. However, widespread interest of the scientific community in tissue engineering was triggered by two phenomenal reviews: one by Nerem [5] on cellular engineering and another by Langer and Vacanti on tissue engineering [6]. These reviews discuss in depth, for the first time, the possibilities of tissue engineering and presented some of the preliminary studies demonstrating proof of the concept. Figure 1.1 shows the process of tissue engineering [7]. The field of tissue engineering has now developed into a highly interdisciplinary science and has attempted to recreate or regenerate almost every type of human tissue and organ [8]. This was possible within a short time due to the highly multidisciplinary nature of the tissue engineering approach, which makes use of the combined efforts of basic and material scientists, cell biologists, engineers and clinicians. Several different definitions for tissue engineering followed the NSF consensus definition due to the interdisciplinary approach and our laboratory defines tissue engineering as ''the application of biological, chemical and engineering principles towards the repair, restoration or regeneration of living tissues using biomaterials, cells and factors, alone or in combination'', describing the different possible approaches for tissue engineering [9]. Thus, three or more approaches are currently used to regenerate tissues using the principles of tissue engineering. One approach is the guided tissue engineering that uses a biomaterial membrane to guide the regeneration of new tissue; another approach called cell transplantation uses the application of isolated cells, manipulated cells (gene therapy) or cell substitutes to promote tissue regeneration. A third approach uses biomaterial in combination with bioactive molecules called growth factors to induce and guide tissue regenera-

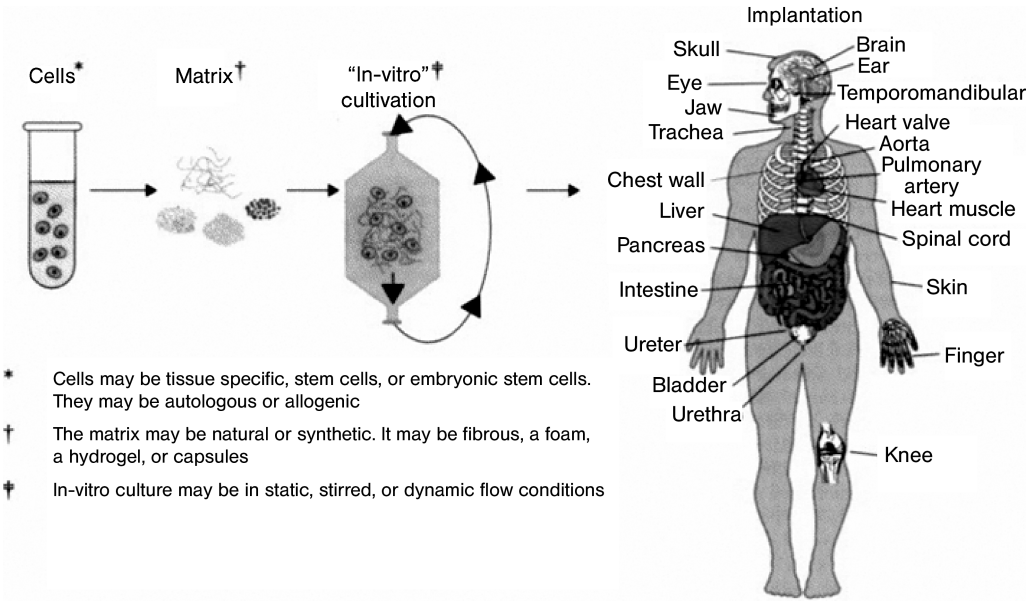

Fig. 1.1. Scheme showing the process of tissue engineering. (Adapted from Ref. [7] with permission from Elsevier.)

tion and a fourth, the most extensively investigated approach, uses biomaterials in combination with cells (with and without biological factors). Within the cell–biomaterial combination approach two different methods are used, a closed system and an open system. In a closed system cells are protected from the immune response of the body by encapsulating in a semi-permeable membrane that can allow nutrient and waste transport to keep them functional. In an open system, the cell–biomaterial construct is developed *in vitro* and is directly implanted in the body. In the open system, biomaterials are used to develop supporting matrices or scaffolds for cell implantation. Bioresorbable polymers (both synthetic and natural polymers) are commonly used for fabricating scaffolds. Several fabrication techniques are used to develop porous 3D scaffolds from these biomaterials. The function of the scaffold is to guide the regeneration of new tissue and to provide appropriate structural support, i.e., to mimic the structure and functions of natural extracellular matrix (ECM). The exogenous cells delivered through the scaffolds along with endogenous cells are used to regenerate or remodel the damaged tissue. During this process the bioresorbable scaffold will degrade and disappear resulting in the formation of remodeled native tissue [8]. Research to date has identified different cell sources, including stem cells that, when combined with degradable, matrices can form 3D living structures. The technique has led to the development of many tissues in the laboratory scale such as bone, ligament, tendon, heart valves, blood vessels, myocardium, esophagus, and trachea. However, several engineering and biological challenges still remain for successful clinical translation of the labo-

ratory research to make tissue engineering a reliable route for organ/tissue regeneration. These include mimicking the complex structure and biology of the ECM using synthetic materials, controlling cell interactions using artificial scaffolds, vascularization of cell–scaffold constructs, development of efficient bioreactors for *in vitro* culture, storage and translation [10]. The present chapter reviews progress made in tissue engineering to overcome some of the engineering and biological challenges in developing ideal 3D synthetic scaffolds by harnessing nanotechnology and material science.

This chapter also overviews the importance of mimicking the structure and functions of the ECM when developing ideal scaffolds for tissue engineering and the recent developments and advantages of nanotechnology assisted techniques to fabricate scaffolds that closely mimic the ECM.

After the present section, which gives a brief introduction to tissue engineering, Section 1.3 lays out the importance of scaffolds in tissue engineering and the need for mimicking the structure and functions of the ECM. Section 1.4 reviews the important aspects of the structure and functions of the ECM that need to be mimicked to develop ideal scaffolds for tissue engineering. Section 1.5 includes in-depth examination of the applications of nanotechnology in developing ECM mimic nanostructured scaffolds for tissue engineering. Section 1.6 reviews some recent studies, demonstrating the advantages of nanostructured scaffolds for tissue engineering, and Section 1.7 overviews some of the current applications of nanostructured scaffolds for engineering different tissues.

1.3 The Importance of Scaffolds in Tissue Engineering

The importance of the extra-cellular matrix (ECM) in cellular assembly and tissue regeneration was demonstrated by the pioneering works of Mina Bissell along with others [11]. The cells in mammalian tissues are connected to the ECM which provide three-dimensionality, organize cell–cell communications and provide various biochemical and biophysical cues for cellular adhesion, migration, proliferation, differentiation and matrix deposition. Their studies have shown the significant differences in behavior of cells when grown in two-dimensional (2D) and 3D environments [11].

Even though 2D cell culture techniques have been extensively used by cell biologists to derive valuable information regarding cellular processes and cell behavior, in the light of recent studies it is evident that *in vivo* tissue response can be simulated only through 3D cell culture techniques [12]. Considering the complex biomechanical and biochemical interplay between cells and the ECM, it is apparent that tissue engineers will be unable to address the biological subtleties if the cells are grown on 2D biomaterials before implantation in the body.

The strategy of using bioresorbable porous synthetic scaffolds as artificial ECM was introduced by Langer and Vacanti in 1988 [13]. This seminal paper significantly influenced investigators throughout the world in the practical area of scaf-

fold based tissue engineering and has led to hundreds of research articles and patents to date.

A bioresorbable α-hydroxyester was used as the candidate polymer in the first study by Langer's group for developing the scaffolds. The α-hydroxyesters being aliphatic polyesters have the ability to undergo hydrolytic degradation *in vivo* and therefore could resorb and disappear once regeneration is complete. Studies that followed have shown that the properties of the biomaterial play a crucial role in the success of the tissue engineered construct. Since the dynamics of different tissues vary significantly, appropriate materials need to be carefully chosen to satisfy the properties required. This knowledge has led to the design and development of several bioresorbable polymeric biomaterials to fabricate scaffolds for engineering different types of tissues [14]. These include synthetic polymers such as α-hydroxyesters, polyanhydrides, polyphosphazenes, polyphosphoesters and natural polymers such as collagen, gelatin, chitosan and hyaluronic acid [15, 16]. Among these, synthetic polymers are mostly preferred for developing tissue engineering scaffolds due to immunogenic problems and batch by batch variations associated with many of the natural polymers.

Apart from the properties of the materials, the 3D architecture of the scaffold is very important when attempting to mimic the structure and functions of the natural ECM. Several unique fabrication processes have been developed to form 3D porous structures from bioresorbable materials as scaffolds for tissue engineering [9, 17]. These 3D structures have been primarily designed to direct tissue growth by allowing cell attachment, proliferation and differentiation. Most of these fabrication processes have been designed based on a set of criteria that have been identified as crucial to promote cellular infiltration and tissue organization. Some of the basic requirements of scaffolds for tissue engineering, summarized by Agarwal and Ray [18], are that they should be:

- Biocompatible.
- Bioresorbable and hence capable of being remodeled.
- Degrade in tune with the tissue repair or regeneration process.
- Highly porous to allow cell infiltration.
- Highly porous and permeable to allow proper nutrient and gas diffusion.
- Have the appropriate pore sizes for the cell type used.
- Possess the appropriate mechanical properties to provide the correct micro-stress environment for cells.
- Have a surface conducive for cell attachment.
- Encourage the deposition of ECM by promoting cellular functions.
- Able to carry and present biomolecular signals for favorable cellular interactions.

Various studies have been performed so far, using macro- and micro-fabrication techniques, to form 3D scaffolds that could address the requirements listed above to develop ideal synthetic scaffolds with some success. The results of these studies have been extensively reviewed [17, 19–23]. Particulate leaching can be considered as one of the first techniques widely used to develop micro-porous matrices from

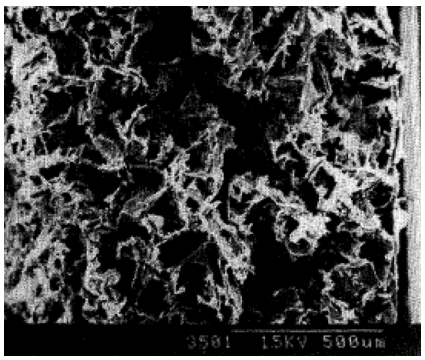

Fig. 1.2. Porous bioresorbable poly(L-lactic acid) foams developed by particulate leaching. (Adapted from Ref. [24] with permission from Elsevier.)

biodegradable polymers for tissue engineering applications (Fig. 1.2) [24–26]. The technique has several advantages such as ease of processing, ability to develop foams from wide range of polymers, and the ability to control the pore size by varying the size of the porogen. However, the porogen leaching process has some serious limitations to fabricate scaffolds for tissue engineering, such as the inability to completely remove the porogen from the porous matrix and to control the pore shape and maintain interconnectivity between pores. Consequently, several modifications to the particulate leaching method as well as new fabrication techniques were developed. Some of the newer processes include sintered microsphere process and rapid prototyping.

Sintered microsphere matrix fabrication technique of Laurencin was developed as a robust technique to fabricate 3D porous structures with reproducible porosities and interconnected pore structure [27, 28]. Sintered microsphere matrices are developed by heat sintering bioresorbable polymeric microspheres (Fig. 1.3)

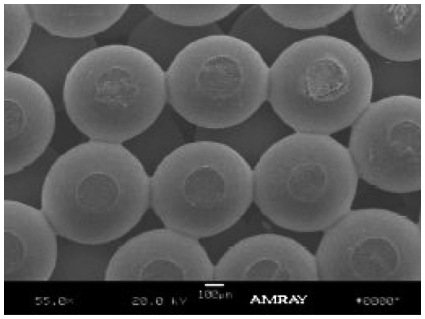

Fig. 1.3. SEM showing the 3D porous structure of a PLAGA scaffold formed by the sintered microsphere fabrication process. (Adapted from Ref. [29] with permission from Elsevier.)

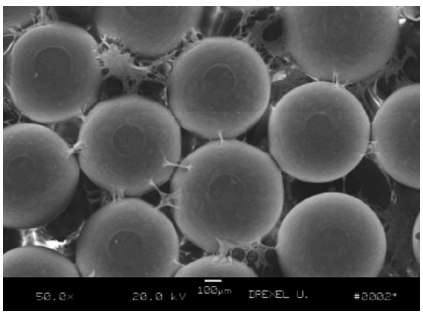

Fig. 1.4. SEM showing human osteoblast attachment and infiltration in porous PLAGA sintered microsphere matrix. (Adapted from Ref. [29] with permission from Elsevier.)

[27, 28]. Poly(lactide-*co*-glycolide)s (PLAGA) having different ratios of lactic acid (LA) and glycolic acid (GA) were used as the polymers to develop sintered matrices. Polymeric microspheres are prepared by the commonly used solvent evaporation technique [27, 28]. The sintered microsphere matrices demonstrated controllable pore size and interconnectivity depending on the size of the microspheres used to fabricate the matrices. Thus, the pore size of the scaffolds could be varied from 100 to 300 µm, depending on the size of the microspheres used. The 3D porous sintered microsphere scaffolds were investigated as potential candidates for bone tissue engineering and showed appropriate mechanical properties for orthopedic applications. The osteoconductivity of the porous 3D matrices were evaluated using human osteoblast cells and showed good osteoblast attachment and infiltration (Fig. 1.4) [28, 29]. An *in vivo* evaluation demonstrated the efficacy of the bioresorbable sintered microsphere matrix in healing a critical segmental bone defect in a rabbit model [30]. Figure 1.5 shows the X-ray of a bone defect site implanted with a sintered microsphere matrix after eight weeks of implantation. The study showed the formation of new bone throughout the entire structure of the implant indicating significant bone regeneration at the defect site. The fabrication process led to the development of porous scaffolds having high interconnectivity and good mechanical integrity, with the percentage pore volume of the matrices equal to ~40%.

Recently, different types of computer-assisted design and manufacturing processes (CAD/CAM) were investigated as potential methods to develop scaffolds

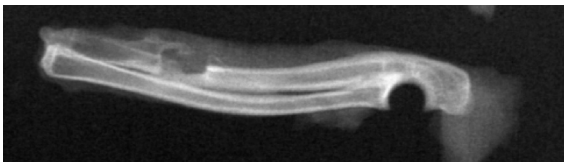

Fig. 1.5. Radiograph of a defect site implanted with sintered microsphere matrix, bone marrow cells and BMP-7 after 8 weeks of implantation, showing significant bone regeneration.

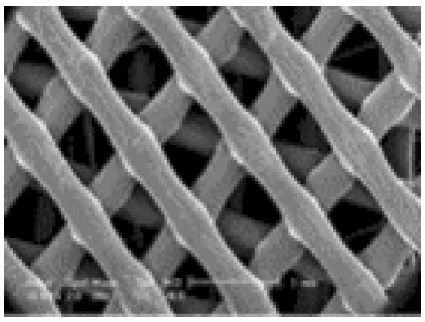

Fig. 1.6. SEM showing the porous structure of a polymer scaffold developed by FDM. (Adapted from Ref. [23] with permission from Elsevier.)

having controllable pore size, shape and porosity. One of the first developed computer assisted techniques for scaffold fabrication was solid free form fabrication or 3D printing. In this process a complex 3D structure is first designed using CAD software. An inkjet printing of a binder on appropriate polymer powder layers is then used to fabricate the porous structure based on the computer model. Even though complex structures can be designed and fabricated using this automated process, the preciseness of the technology has various limitations imparted by the size of the polymer particle, size of the binder drop and the type of the nozzle tip [31]. Another rapid prototyping technique extensively investigated for developing porous scaffolds for tissue engineering is fused deposition model (FDM) developed by Hutmacher [22, 23]. The FDM can be used to develop 3D structures from a CAD or an image source such as computer tomography (CT) or magnetic resonance imaging (MRI) of the object. The computer design is then imported into software that mathematically slices the model into different horizontal layers. The FDM extrusion head and the platform are then synchronized to deposit fused polymeric melt based on the computer model, one layer at a time. Figure 1.6 shows a porous 3D structure developed from a bioresorbable polymer poly(caprolactone) (PCL). The FDM process has several advantages, such as the ability to precisely control the pore size, pore morphology and pore interconnectivity. The process enables also the development of multiple-layer designs and different localized pore morphologies needed for multiple tissue types or interfaces. Another advantage of FDM is the good mechanical properties and structural integrity of the scaffolds due to the use of mechanically stable designs and proper fusion between individual material layers. However, the fabrication process has some limitations that make it less than an optimal method for developing porous matrices for tissue engineering applications. These include the limitations associated with the processing technique such as the requirement of temperature, the need for materials that are appropriate for fused deposition, the necessity of supporting structures to construct complex structures, and variable pore openings observed along different axis [32].

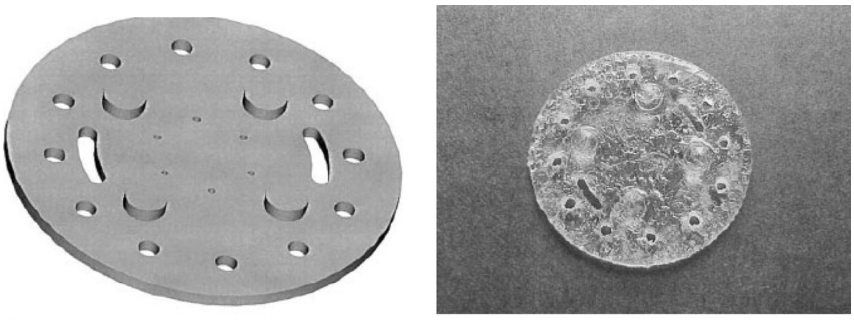

A B

Fig. 1.7. (A) Pro/Engineer rendered CAD image of prototype PPF construct. The series of slots and projections test the interslice PPF registration (50 × 4 mm). (B) Three-dimensional structure developed from CAD model data from PPF. (Adapted from Ref. [33].)

Several stereolithographic techniques were investigated to develop porous 3D matrices from polymers to overcome the problems associated with temperature-assisted fabrication methods. Stereolithographic techniques have been extensively used to develop 3D structures from photopolymerizable polymer solutions such as poly(propylene fumarate) (PPF) in presence of photoinitiators (Fig. 1.7A and B) [33]. Preliminary studies showed the feasibility of developing structures having controlled pore sizes (50–300 μm) and different layer thicknesses using a highly controlled laser light source.

Most of the techniques described above are used to develop 3D structures from synthetic hydrophobic polymers. However, a wide range of techniques using hydrophilic polymers have also been investigated to develop novel structures as cell delivery vehicles. Hydrophilic polymers are good candidates to develop tissue engineering scaffolds due to their high water content and ability to mimic the properties of various tissues. One such technique is the use of photolithography to pattern hydrogel films with hydrophilic porous structures [34].

The fabrication techniques discussed so far have been developed to fabricate acellular scaffolds that are populated with appropriate cells after fabrication for tissue engineering applications. However, this process has the limitation of obtaining uniform cell distribution throughout the scaffold even with the use of bioreactors during *in vitro* culture. Therefore some studies have also focused to develop materials and fabrication processes to form cellular scaffolds. These studies have led to the development of different types of stimuli sensitive hydrophilic polymers that can be used to encapsulate cells under mild conditions to form cellular scaffolds [35, 36]. Cells can be uniformly distributed in the aqueous stimuli sensitive polymer solutions before the gelling process (Fig. 1.8) [37]. Attempts are currently underway to combine this process with the lithographic techniques to form cell incorporated 3D structures under very mild conditions.

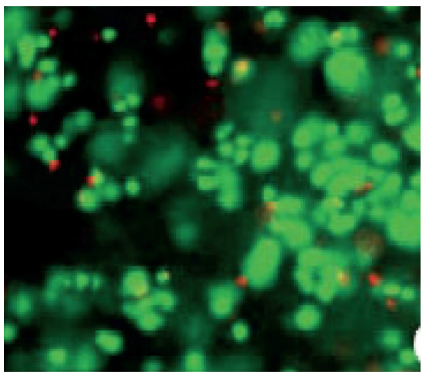

Fig. 1.8. Photomicrograph showing chondrocytes encapsulated within a hydrogel after 21 days in culture stained using Live dead stain (green shows live cells and red shows dead cells). (Adapted from Ref. [37] with permission from Elsevier.)

Another strategy recently developed to form structures with uniform distribution of cells throughout the scaffold is cell printing [38]. This approach combines rapid prototyping procedures with microencapsulation to print viable free form structures using bio-ink with custom-modified ink-jet printers. One advantage is the feasibility of placing quickly and precisely various cells layer by layer to develop multi-cell systems. However, the process is still in its infancy and further research is necessary with regards to developing appropriate bio-ink, optimizing the rheologic and surface properties of the inks, and designing printers optimized for these properties [39]. Another strategy is organ printing, which makes use of nature's ability to assemble many tissue forms such as blood vessels. The technology is based on the hypothesis that when cell aggregates are placed in close approximation they can assemble to form a disc or tube of tissue (Fig. 1.9) [40–42]. This process is also still in its infancy, has various scaling up limitations and further studies are needed to demonstrate the potential of the approach.

The previous discussion demonstrates the importance of the ECM in tissue repair and regeneration and serves as a brief overview of the attempts made to mimic the structure of the ECM using polymeric biomaterials and various macro/micro fabrication techniques to develop interconnected porous structures having porosities in the micron range. These studies have led to the design and synthesis of novel bioresorbable materials with unique chemistries, fabrication of 3D structures having different properties and demonstrated the feasibility of growing cells in appropriate 3D forms *in vitro* and *in vivo* with the help of these scaffolds. Figure 1.10(A and B) shows the feasibility of developing an artificial ear on the back of a mouse using a bioresorbable PCL scaffold having the macroscopic shape of an ear seeded with chondrocytes [43].

Even though these materials and fabricated 3D structures showed the feasibility of 3D organization of cells into tissue, they are far from being ideal for develop-

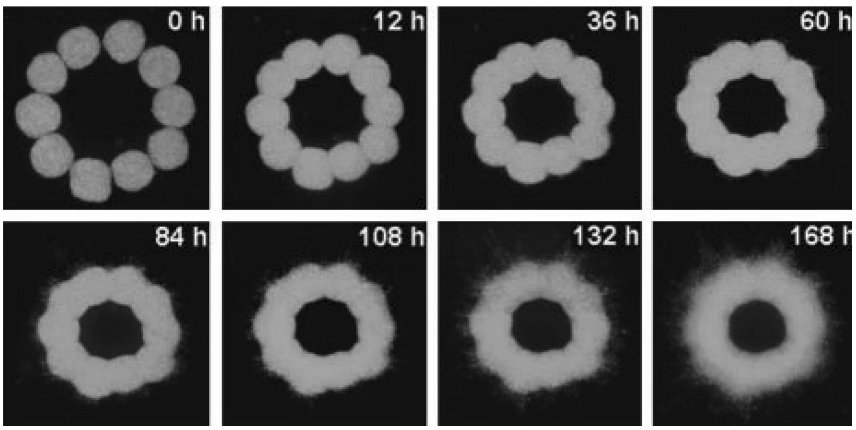

Fig. 1.9. Time evolution of the fusion of aggregates of Chinese Hamster Ovary (CHO) cells encapsulated in collagen gel. The nuclei of the cells are fluorescently labeled. Cell before fusion (top left) and the final disc-like configuration after fusion (bottom right). (Adapted from Ref. [37] with permission from the National Academy of Sciences, USA.)

ing fully functional tissues and organs *in vivo* in a reproducible way under clinical setting.

So far, most of the biomaterial design has focused on developing materials that are capable of degrading at a rate that matches tissue regeneration, have the ability to degrade into non-toxic degradation products and can support the adhesion and proliferation of cells without placing much emphasis on the bioactivity of the materials. Conversely, most fabrication techniques are focused on developing scaffolds with macroscale properties, such as the ability to provide sufficient transport prop-

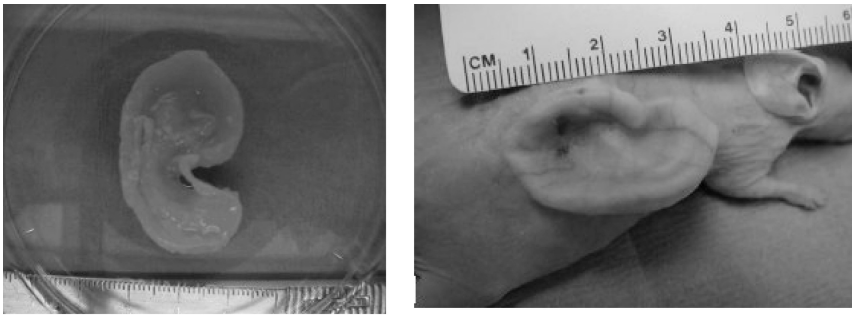

Fig. 1.10. (A) Photomicrograph of tissue engineered ear construct developed from chondrocyte-PCL composite after 8 weeks *in vitro* culture. (B) The regenerated ear on the back of athymic mice. (Adapted from Ref. [43] with permission from Elsevier.)

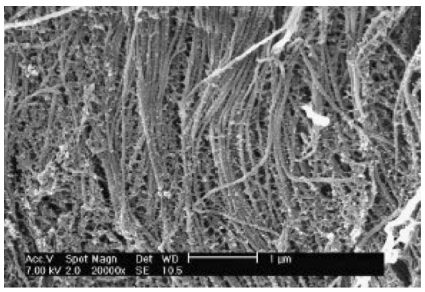

Fig. 1.11. High magnification picture of collagen fibrils in human aortic valve. Individual fibrils are separated by a narrow space crossed by interfibrillar bridges formed by small proteoglycans interconnecting adjoining fibrils. (Adapted from Ref. [44] with permission from Elsevier.)

erties (interconnected microporous structure), and adequate mechanical properties (to match the properties of the tissue to be replaced or repaired).

However, the organization of the cells, and hence the properties of the tissue, are highly dependent on the structure of the ECM, which has a hierarchical structure with nano-sized features. Figure 1.11 shows the ultrastructure of collagen fibrils in human aortic valves, illustrating the nanoscale topographic features of the native tissue [44]. Thus, successful fabrication of a fully functional tissue is a far more complex and involved process that requires the creation of an appropriate environment at both a micro- and nano-scale level to allow for cell viability and function along with macroscopic properties [45]. In fact, just as important as these structural features are the biological principles that govern cell–cell and cell–matrix interactions. These interactions form the basis of cellular performance and appropriate tissue organization and are controlled by various biochemical cues present in the natural ECM. The recreation of this process requires the incorporation of various bioactive molecules in synthetic porous scaffolds with molecular precision to mimic the functions of the ECM. Recently, a paradigm shift has been observed from developing macro/micro-structured scaffolds to nanostructured bioactive scaffolds in an attempt to improve tissue design and reconstruction in reparative medicine [46, 47].

1.4
Structure and Functions of Natural Extracellular Matrix

Since the ultimate goal of tissue engineering is to develop tissue substitutes that could temporarily mimic the structure and functions of damaged tissue to be replaced, it is crucial that the engineered substitutes mimic the natural tissue structurally and functionally for successful regeneration. Extensive research performed in different areas such as tissue and organ development during embryogenesis, the

normal tissue healing process, tissue structure and functions and development of various characterization techniques at the micro- and nano-scale levels have significantly enhanced our ability to mimic native tissue. The human body is a very complex structure that is organized in a hierarchical way with body composed of systems, systems composed of organs, organs composed of tissues and tissues composed of cells, vasculature and extracellular matrix. In tissues, the ECM provides the structured environment with mechanical and biochemical cues that enable the cells to interact with each other and with the ECM to allow for control of growth, proliferation, differentiation and gene expression.

The ECM is composed of a physical and chemical crosslinked network of fibrous proteins and hydrated proteoglycans with glycosaminoglycan side chains (collectively called the physical signals) in which other small molecules (such as growth factors, chemokines and cytokines) and ions are bound. Figure 1.12 shows the ultrastructural features of an ECM with a condensed basement membrane and the stromal tissue [48]. The ECM proteins are mainly composed of more than 20 different types of collagens as well as elastin, fibrillin, fibronectin, and laminin [49]. In the natural environment these macromolecular ECM components are secreted by the cells and then modified and assembled to form the matrix during the tissue development and repair process. Among the ECM proteins, type I collagen is mainly involved in the formation of the fibrillar and microfibrillar structure of the ECM. Type I collagen molecules (~300 nm long and ~1.5 nm in diameter) are packed to form collagen fibrils. Each collagen fibril displays a characteristic

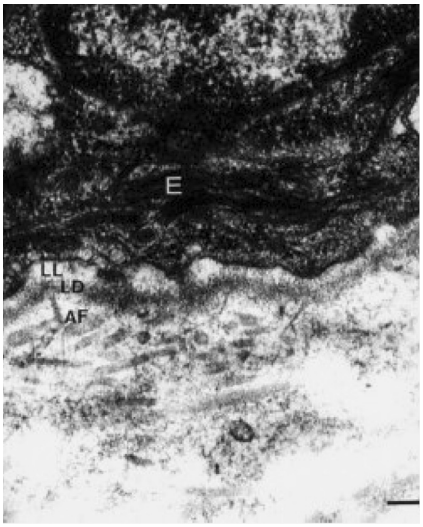

Fig. 1.12. Ultrastructure of ECM matrix. Adjacent to an epithelial cell (E) is the basement membrane with its amina lucida (LL) and lamina densa (LD). The interstitial matrix contains collagen fibrils and is close to the basement membrane anchoring fibrils (AF), composed of type VII collagen fibrils. (Adapted from Ref. [48].)

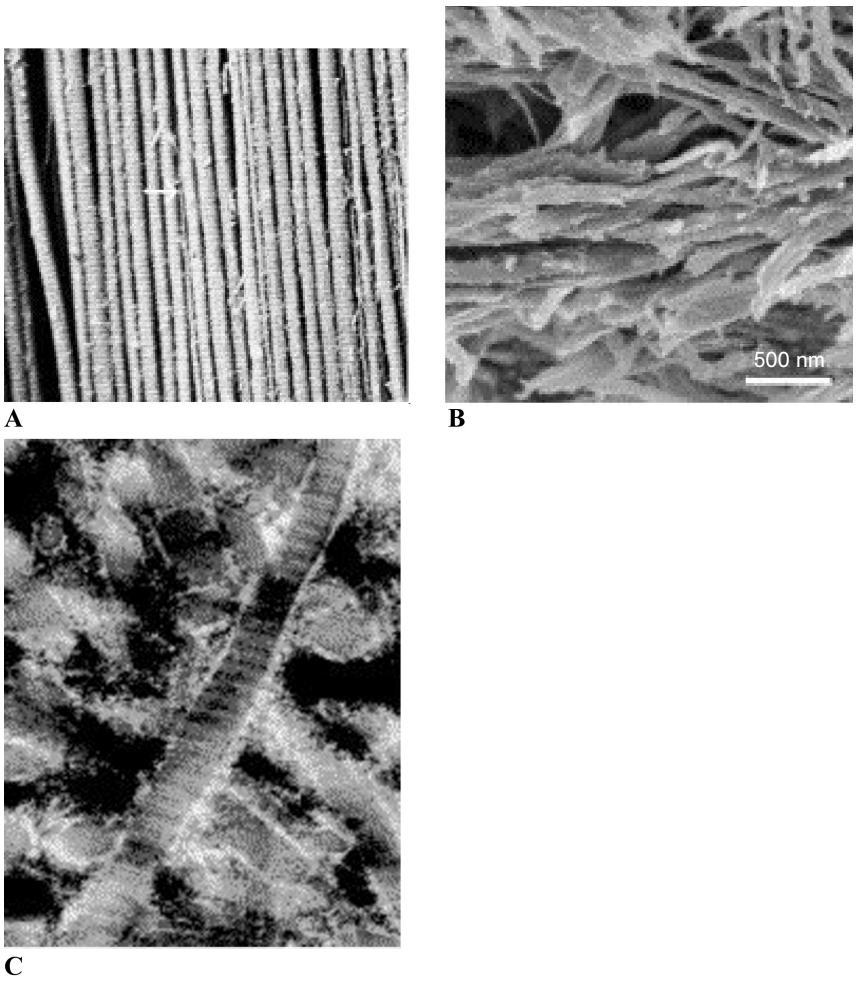

Fig. 1.13. Structure and orientation of collagen fibrils of various tissues. (A) Mature rat ligament-collagen fibrils are primarily aligned along the long axis of the ligament. (Adapted from Ref. [51] with permission from Elsevier.) (B) Mineralized fibrils in trabecular bone without the non-fibrillar matrix. (Adapted from Ref. [52] with permission from Elsevier.) (C) Articular cartilage. (Adapted from Ref. [53] with permission from Elsevier.)

~67 nm D-repeat with uniform or multi-model diameter distribution varying from ~25 to 500 nm and several micrometers in length, depending on the nature of the tissue. All of these molecules are arranged in a unique tissue specific 3D architecture [50]. Figure 1.13 shows the different arrangement patterns of collagen fibrils as observed in three different types of tissues (A: ligament; B: bone; and C: articular cartilage) [51–53]. Fibrils show varied orientation in different tissue types that give the appropriate physical and mechanical properties to the tissue. Collagen fi-

brils are further bundled together to form collagen fibers. The hierarchical structure of the ECM has length scales, varying from a few nanometer (nm) to millimeter (mm) that control the cellular functions and corresponding tissue properties. The fact that cells are highly sensitive to the environmental structural features has been demonstrated using *in vitro* cell culture studies on nanopatterned surfaces fabricated by electron beam lithographic techniques. These studies revealed that the cells are sensitive to nanoscale dimensions and could react to objects as small as 5 nm [54]. This can be attributed to the structural details ECM presents to the cells *in vivo*. Thus, the 3D hierarchical structure of the ECM significantly affects cellular behavior and hence tissue functions through topographical cues.

However, the function of the ECM is not just to provide an inert support for cellular adhesion. Almost all of the molecules present in ECM have both structural and functional roles. The ECM serves mainly to organize cells in space to give them form, provide them with environmental signals, to direct site-specific cellular regulation, and separate one tissue space from another. Thus the orientation and position of cells with respect to each other is dictated by the ECM and the orientation varies with different tissues. This is achieved by providing chemical cues such as insoluble signals or factors of the ECM which could interact with the soluble signals of cells along with the structural features to promote adherence, migration, division and differentiation of cells. In a natural tissue the ultimate decision of cellular processes such as adhesion, proliferation, differentiation, migration and matrix production takes place as a result of this continuous cross-talk between cells and ECM effectors [55]. Figure 1.14 shows a schematic representation of various interactions taking place between cells and ECM during tissue organization and function [50].

At least three mechanisms have been identified though which the ECM can regulate cell behavior. The first mechanism is through the composition of the ECM such as various proteins and glycosaminoglycans, which is highly tissue and cell specific. The second mechanism is through synergistic interactions between growth factors and matrix molecules. The growth factors are found to bind with the ECM through the glycosaminoglycan side chains or protein cores and this increases the stability of growth factors and creates the appropriate cellular environment or niche to regulate cell proliferation and differentiation. The third mechanism is through the cell surface receptors or integrins that mediate cell adhesion to extracellular matrix components [56]. The integrin–ECM ligand interactions play a major role in anchoring cells to the ECM. An integrin is ∼280 Å long and consists of one α (150–180 kDa) and one β (∼90 kDa) subunit, both of which are type I membrane proteins [57]. About 18α and 8β subunits that can form 24 different heterodimers have been identified so far and the ligand specificity of the integrin is determined by the specific $\alpha\beta$ subunit combination [58]. Integrin-mediated cell adhesion to the ECM occurs through a cascade of processes. First cell attachment occurs where cell attach to the surface with ligand binding through integrins to withstand gentle shear forces followed by cell spreading. Next organization of actin into microfilament bundles or stress fibers occurs. In the last stage the formation of focal adhesion occurs, which links the ECM to molecules of the actin

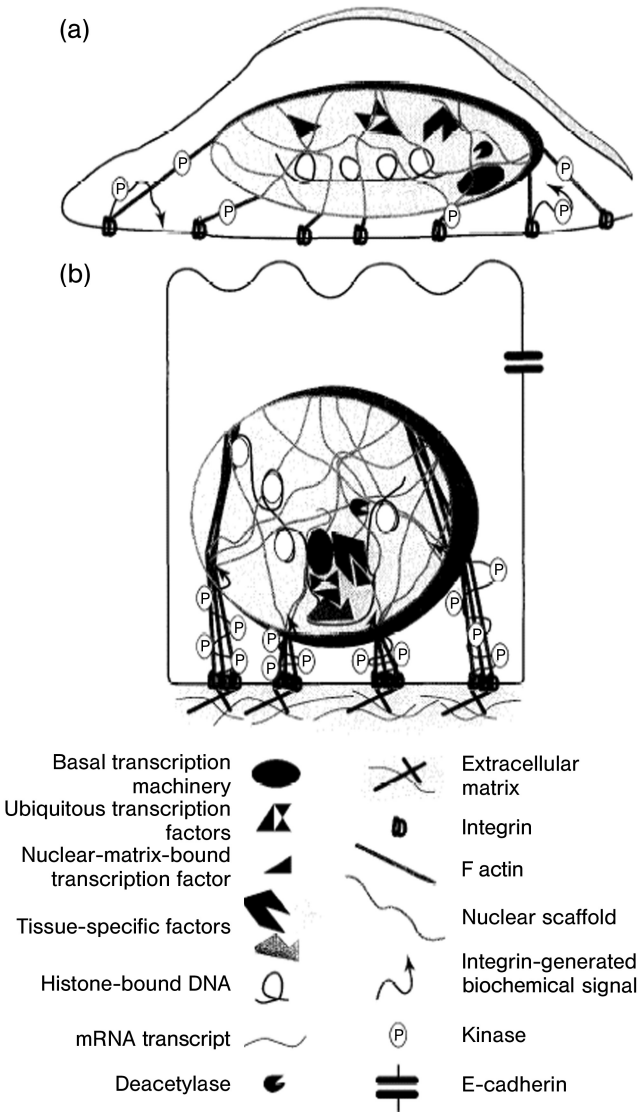

Fig. 1.14. Scheme showing the various interactions between cells and the ECM during tissue organization and repair. (a) Flattened cells in the absence of ECM. Due to incompatible cytoskeletal organization no signals originating from integrin receptors can be properly propagated. (b) In the presence of ECM, binding of ECM components to integrin receptors induces integrin clustering and generates biochemical signals. Cytoskeleton filaments intimately associated with the cytoplasmic domains of the integrins are modified and reorganized to facilitate interaction of the incoming signals with downstream mediators. This reorganized cytoskeleton can evoke further architectural changes via its association with the nuclear matrix. The subsequent nuclear reorganization brings together incoming signaling molecules, transcriptional activators, histone deacetylases, and the basal transcriptional machinery to promote the assembly of a functional transcriptional complex on the gene. (Adapted from Ref. [50] with permission from Elsevier.)

cytoskeleton. The focal adhesion is mainly composed of clustered integrins and other transmembrane molecules. In this process, the integrins have two-fold activities, anchoring the cells to the ECM and signal transduction through the cell membrane [59]. This allows for continuous cross-talk between ECM and cells which is highly crucial for proper tissue functioning [60].

Several studies have been performed to characterize and analyze the largest and most stable types of contacts between the ECM and cells. These include focal adhesions, focal contacts or adhesion plaques, fibrillar adhesions and hemidesmosomes (Table 1.1) [61]. Several morphological criteria have been used to characterize the

Tab. 1.1. Characterization of cell–matrix contact structures. (Reprinted from Ref. [61] with permission from Birkhäuser Verlag, Basel.)

Contact type	Dimensions	IRM Image separation from substratum	Characteristic associations
Close contact	(Associated with lamellipodium)	Grey in IRM 30–50 nm from substratum	Submembranous densities parallel to F-actin meshwork at plasma membrane
Filopodium	20–200 μm long 0.2–0.5 μm diameter	grey in IRM	core bundle of F-actin, integrins, syndecans
Focal contact/focal adhesion/	0.25 μm wide 1.5 μm long	Black in IRM 10–15 nm from substratum	At termini of microfilaments, contain integrins, syndecan-4, low tensin content
Hemidesmosome	Plaque ca. 0.15 μm by 0.04 μm	–	Connect to intermediate filaments, contain $\alpha 6\beta 4$ integrin, plectin, BP230
Matrix assembly sites/fibronexus/ fibrillar adhesions	ca. 3–5 μm long	White in IRM 100 nm from substratum	ECM cables align parallel with microfilaments, contain $\alpha 5\beta 1$ and tensin
Podosomes	0.2–0.4 μm diameter	Dark in IRM	Core bundle of act in perpendicular to substratum, in macrophages contain $\beta 2$ integrins, fimbrin
Spike or microspike	2–10 μm long 0.2–0.5 μm diameter	Grey in IRM	Core bundle of F-actin, contain fascin

contact type and size of the contact including evaluation of phase-dark structures detected by phase contrast or interference reflexion microscopy (IRM), electron-dense and organized structures detected by transmission electron microscopy and cell surface topography detected by scanning electron microscopy (SEM) [61]. Table 1.1 shows that even though the size of a cell is ~10 μm, the activities leading to cell adhesion and the following processes take place mainly at the nanometer level.

Detailed studies on integrin-mediated cell adhesion to the ECM clearly point to the importance of ECM ligands on cell behavior. In addition to the structure and size of the ECM–cell contact points, several studies have been performed to elucidate the biological molecules involved in the interactions. The results of these studies have significantly influenced tissue engineers and have become a great tool in their attempts to recreate a natural cellular environment using synthetic scaffolds. Many of the identified biological molecules have been utilized to decorate synthetic scaffolds to form ligand-functionalized matrices to increase their bioactivity. Various surface modifications or one-dimensional nanotechnological modifications are used to develop ligand functionalized scaffolds [62].

Several cell recognition motifs such as fibronectin, vitronectin, collagen and laminin present in the natural ECM have been used to modify the surface of biomaterial scaffolds to increase their bioactivity [63–65]. Even though preliminary studies show significant promise in developing biomimetic scaffolds, the modification of matrices using bioactive proteins has several limitations. Proteins are bioactive molecules and can elicit an immunological response as they are mostly isolated from different sources and also possess the risk of associated infections. Another serious limitation associated with protein surface modification is that the surface topography and chemistry of the synthetic matrix could influence the orientation and conformation of the attached or adsorbed protein, thereby affecting its functionality. Owing to the low stability of the proteins, the immobilization process as well as subsequent storage could also affect its patency.

The breakthrough research that revolutionized the biomimetic surface modification approach towards biomaterials development is the finding that low molecular peptides from ECM proteins such as the tetrapeptide "arginine-glycine-aspartate-serine" (GRGDS) sequence could significantly modulate cellular behavior [66, 67]. Following this, several RGD-containing sequences were found in other ECM proteins and several other short linear adhesive sequence motifs have also been identified as active molecules to promote cell adhesion, proliferation and migration. Several studies have been performed to elucidate the mechanisms by which these sequences could interact with cells. The tetrapeptide and tripeptide sequences such as arginine-glycine-aspartate can bind to members of the integrin family of the transmembrane receptors, thereby activating a series of signaling events within the bound cells favorably affecting their functions [67–72]. The RGD sequence has been quickly identified as a potential candidate to develop biomimetic scaffolds and extensive research has followed. Because the RGD sequence is present in multiple ECM proteins such as fibronectin, laminin, collagen and vitronectin, a broad range of cell types could respond to this peptide sequence. Furthermore, small peptide sequences are highly stable compared to the corresponding proteins [73], they

are cost effective [74], can be packed densely on surfaces due to their small size, and can selectively address one type of cell adhesion receptors for controlled cell adhesion during multicellular tissue development [68].

Various techniques have been attempted to immobilize these biological motifs on synthetic biomaterial surfaces to increase their bioactivity [75]. Stable immobilization of these ligands to the surface is crucial for proper functioning, as the peptide sequence should be able to withstand the cells contractile forces during initial attachment and prevent internalization by cells [76, 77]. The most extensively investigated approach to covalently immobilize the RGD sequence on surfaces is by using active functional groups such as hydroxyl, carboxyl or amino groups on the RGD and polymer surfaces, involving carbodiimide chemistry [75]. For polymers devoid of these functional groups, several approaches were attempted, such as coating the surface with a polymer having such active groups such as polylysine [75, 78] and coating with RGD modified pluronics via hydrophobic interactions [75, 79]. Another approach to incorporate active groups is by copolymerizing with a monomer having active groups such as acrylic acid [75, 80] or lysine in the case of poly(lactic acid-*co*-lysine) [75, 81]. Another extensively investigated approach is chemical or physical surface modification of biomaterials such as alkaline hydrolysis [75, 82], oxidation [75, 83], reduction [75, 84], etching [75, 85] or plasma deposition [75, 86].

Even though immobilization via carbodiimide chemistry is a versatile approach to covalently immobilize RGDs on various surfaces, it is not a highly selective process as RGD has two reactive groups (amino and carboxyl) and therefore can lead to various un-wanted side reactions. A recent study has demonstrated the feasibility of incorporating RGDs on the surface of polymers without the various functionalization routes described above. The approach is called chemoselective ligation. Under mild conditions, selected pairs of functional groups are used to form stable bonds with RGD without interfering with other functional groups [87]. Thus thiol-functionalized surfaces can be modified using bromoacetyl containing RGD cyclopeptides [88] or a thiol-containing RGD can be linked to maleinimide-functionalized surfaces under mild conditions [89]. Benzophenone or aromatic azide functionalized RGD has been developed as a versatile technique to immobilize RGDs on the surface [90–92] by streptavidin–biotin capture [93].

In addition to direct linking, attachment of RGD to surfaces using spacers significantly increases the activity of immobilized RGDs. This increased activity has been attributed to the ability of RGD peptide binding site to reach the hollow globular head of an integrin. Several studies have confirmed a spacer length of 35–40 Å is optimal for maximum activity [75, 94]. However, recent studies on the crystal structure of the ligand bound extracellular domain of the $\alpha V\beta 3$ integrin show the RGD binding site on the surface region of the head of the $\alpha V\beta 3$ integrin, suggesting that it is only a few angstroms deep [71]. This indicates that spacers may not be needed for the ligand–integrin interaction. The experimental improvement in activity of RGDs with spacers found in some studies has been attributed to the spacer presumably contributing to the surface roughness of the substrates [75].

All of these approaches have shown the feasibility of covalent attachment of

RGDs on the surface of polymeric biomaterials and several studies were also performed to demonstrate the bioactivity of RGD immobilized surfaces. Numerous polymers, various immobilization techniques, different RGD peptides and different cell types were used to investigate the biological activity of biomimetic surfaces. The cell behavior towards RGD modified surfaces has been found to depend on various parameters such as the structure and conformation of RGD as well as the density and arrangement of RGD on the surface. Some of the RGD peptides investigated include RGD, RGDS, GRGD, YRGDS, YRGDG, YGRGD, GRGDSP, GRGDSG, GRGDSY, GRGDSPK, CGRGDSY, GCGYGRGDSPG, and RGDSPASSKP peptides [75]. One study systematically investigated the cell attachment activity of different types of RGDs including RGD, RGDS (from fibronectin), RGDV (from vitronectin) and RGDT (from collagen) immobilized on polymeric surfaces. The study demonstrated that tetrapeptides show distinct increases in cell attachment compared to tripeptides indicating that peptides with higher integrin affinity bear higher cell attachment [80]. No significant differences in cell attachment between the tetrapeptides were observed [80]. Another study showed that cyclic RGD peptides on surfaces can show higher activity than linear molecules, which has been attributed to their higher stability and increased $\alpha v\beta 3$ binding of cyclic peptide compared with linear molecules [95].

Another unique application of RGD modified biomaterials is the development of materials that can promote selective adhesion of various cell types. Since it has been found that each cell type has its own typical pattern of different integrins, RGD peptides could be used to promote selective cell adhesion on a surface by modifying the surface with an appropriate RGD [69]. Some *in vitro* studies have demonstrated the feasibility of integrin specificity of RGD leading to selective cell adhesion on RGD modified surfaces [69]. The study showed that fibroblasts rather than endothelial cells preferably adhered to a RGDSPASSKP (which is selective to $\alpha 5\beta 1$) modified surface [96]. Similarly, enhanced fibroblast attachment was observed to an $\alpha 5\beta 1$ integrin selective GRGDSP peptide functionalized surface where as $\alpha 5\beta 3$ selective cyclic G*PenGRGDSPC*A supported higher smooth muscle cell and endothelial cell densities [97]. However, no data is currently available to show if such modification holds for more complex *in vivo* environments since cells could express more than one type of integrin and also because the integrin expression pattern of a cell is a highly dynamic phenomenon.

The surface density of RGD on the material also has a profound effect on the number of cells attached as well as cell spreading, cell survival, focal contact formation and to some extent proliferation. Studies have shown a sigmoidal increase in cell attachment with RGD concentration on the surface, indicating a critical minimum density for cell response [94]. Thus Neff et al. demonstrated that maximum proliferation of fibroblast occurred on surfaces with intermediate surface concentration ($\sim$1.33 pmol cm^{-2}) [79]. Another study by Massia and Hubbell using RGD functionalized glycophase glass surface has shown that a minimal amount, as low as 1 fmol RGD peptide cm^{-2}, is sufficient for cell spreading on the surface and as low as 10 fmol cm^{-2} sufficient for formation of focal contacts and stress fibers [98].

However, a higher RGD peptide concentration requirement has been reported for polymers and has been attributed to the entropic penalty that results from attachment of a peptide to flexible polymer chain compared to a rigid glass surface as well as the inefficient transmission of forces through polymer surfaces [75, 99]. Studies have shown that in addition to surface concentration, the mode of presentation of ligands also could affect integrin behavior [100]. One study by Maheshwari et al. evaluated surfaces with controlled overall peptide density and controlled nanoscale spatial ligand distribution with an overall RGD distribution of 0.15–20.50 nmol cm^{-2} [101]. The results demonstrated that a significantly higher fraction of fibroblasts showed higher shear stress resistance and exhibited well-formed stress fibers and focal contacts when the ligand was presented in a clustered versus a random individual format. The use of a higher affinity peptide GRGDSPK afforded a lower RGD density of 0.06–0.88 nmol, showing that activity of the RGD is also very important [102].

Nanoscale RGD clustering on the surface of biomaterials seems to be a promising approach to elicit favorable cell responses with minimal amounts of RGD peptides. Studies are ongoing to determine the technique that could be used to create nanoscale clustering on the surface as well as to determine which arrangement elicits a particular cell response.

Thus the foremost challenge in developing a tissue engineered construct is the development of a resorbable synthetic microenvironment that could closely mimic the complex hierarchical micro-nano architecture of the ECM along with the molecular level spatial organization of biological cues found in native tissue *in vivo*.

1.5 Applications of Nanotechnology in Developing Scaffolds for Tissue Engineering

Nanotechnology has been defined as ''research and technology development at the atomic, molecular and macromolecular levels in the length scales of approximately 1–100 nm range, to provide a fundamental understanding of phenomena and materials at the nanoscale and to create and use structures, devices and systems that have novel properties and functions because of their small and/or intermediate size'' [103]. Nanotechnology has emerged as an exciting field that deals with both the design and fabrication of structures with molecular precision. Nanotechnology enables the control and manipulation of individual constituent molecules/atoms to have them arranged to form the bulk macroscopic substrate. The uniqueness of the nanotechnological approach is that it considers spatial and temporal scales at the same time, thereby forming an excellent technique to develop hierarchical structures. The biological milieu that tissue engineers attempt to mimic using synthetic materials and techniques is a highly complex system with spatial and temporal levels of organization that span several orders of magnitude, with different levels nested within higher order levels (nm to cm scale). To study and mimic this complex system, highly sophisticated technology is required. For instance, the

visualization and characterization of these biological structures, processes, and their manipulation require sophisticated imaging and quantitative techniques with spatial and temporal control at or below the molecular level.

Recent developments in nanotechnology have revolutionized the visualization and characterization of biological processes in various ways. The capability of imaging living cells after implantation is very crucial in studying cell behavior and processes *in vivo*. The recent developments in nanotechnology assisted fluorescent probes such as quantum dots (QD) have significantly improved our capability of *in vivo* imaging. QDs are nanocrystals or nanoparticles with size ranging from 1 to 10 nm with unique photophysical and photochemical properties not available with conventional organic fluorophores [104].

Similarly, the scanning probe microscopic techniques (SPM) provide a great tool to investigate atomic and molecular level biological phenomena even though its potential in biology is yet to be realized. One of the most extensively investigated SPM techniques for tissue engineering application is atomic force microscopy (AFM). AFM has provided various strategies to investigate the interactions of living cells with the ECM [105]. AFM has also enabled the visualization of nano-scale biomolecules and significantly contributed to the in-depth understanding of their structure and role in biological process [106].

The developments in current nanoscale fabrication techniques have also significantly increased our understanding of nanoscale features on cellular behavior and tissue organization. Several nanoprinting/etching/electron beam lithographic techniques have been developed to form substrates with large areas of controlled nanoscale features. *In vitro* studies using these substrates confirmed the importance of nanoscale topography of scaffolds for developing tissue *in vitro* [107–110]. One study examined the interaction of fibroblasts with nanoscale islands having heights varying from 10 to 95 nm on polymer films. The fibroblasts underwent rapid organization of cytoskeleton and improved adhesion during initial reaction to the islands with concomitant cell spreading. The lamellae of the cells on the islands also showed many filopodia showing better interaction with the islands. Another study by Dalby et al., using nano- and micro-patterned surfaces has demonstrated the importance of nanoscale features in modulating human mesenchymal bone marrow stromal cell (HBMSC) adhesion [111]. HBMSCs were found to be well-spread and attained normal morphologies on polymer thin films similar to the morphology cells attained on flat topographies. However, the cells on nanofeatured surfaces were found to respond to the nanofeatures. This included cells conforming to the shape of the nanosized pits (Fig. 1.15A – 310 nm deep and 30 μm wide), filopodia production, contact guidance and production of endogenous extracellular matrix. On nanometer depth grooves, the cells were found to be highly aligned along the groove direction showing pronounced contact guidance (Fig. 1.15B – 500 nm deep and 5 μm wide). The study demonstrated that the nanoscale features of the substrates could elicit significant control over cell adhesion, cytoskeletal organization, cell-growth, and production of the osteoblastic markers osteocalcin and osteopontin [111].

To recreate structures having features at the nanoscale level, novel nanotech-

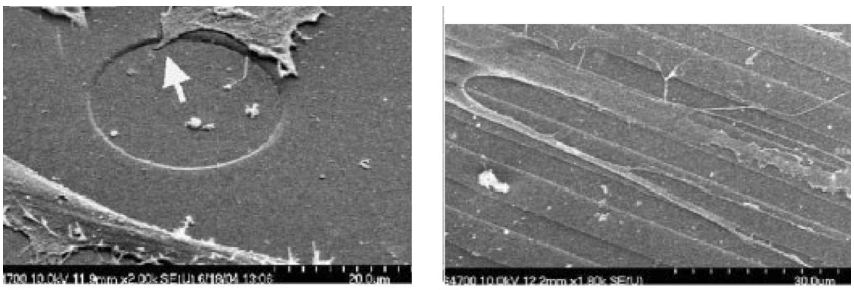

Fig. 1.15. Scanning electron micrographs of HBMSCs cultured on polymer surface with pits and grooves having nanometer depth. (A) Cells conforming to a groove edge of a nanopit (arrow). (B) Contact guidance of cells and their filopodia on the narrow grooves. (Adapted from Ref. [111] with permission from Elsevier.)

niques that enable the conversion of existing macromolecules into nanostructured forms or development of novel structures from atomic or molecular constituents with spatial organization of biofunctionality are needed. It is presumed that these developed nanostructures, due to their ability to interact with cells and tissues at a molecular (subcellular) level with a high degree of functional specificity, would allow a greater extent of integration than previously attainable. Thus, research in this direction is ongoing to develop structures that could temporarily mimic the structure and functions of the ECM as ideal scaffolds for tissue engineering using various nanofabrication processes.

Nanofabrication techniques have shown the feasibility to develop nanostructured scaffolds that better mimic the structure of the ECM compared to the structures developed by macro/micro fabrication techniques. Two different approaches are currently under investigation to develop synthetic nanostructured scaffolds that could resemble the structure of nanoscale collagen fibrils of the ECM as scaffolds for tissue engineering. The first approach can be considered as a ''top-down approach'' which uses synthetic polymeric materials to develop nanostructures using various nanofabrication processes. The second approach can be considered as a ''bottom-up approach'' and is based on short peptides or block polymers that can assemble into nanofibers by a self-assembly process.

1.5.1 Polymeric Nanofiber Scaffolds

As discussed earlier, collagen fibrils are the major building blocks of the natural ECM and they have diameters in the range 50–500 nm and orientation in different directions depending on the tissues. A logical method to develop scaffolds for tissue engineering is to mimic the structure of collagen fibrils, i.e., by using synthetic polymeric nanofiber matrices. Developments in nanofabrication techniques have

enabled the fabrication of synthetic nanofiber matrices from a wide range of polymers. Polymeric nanofibers have been defined as fibers having diameters less than 1 μm and are developed from synthetic and natural polymers [112]. Fibers with diameters ranging from 1–1000 nm and a very high surface area can be developed by the nanofabrication processes. Thus a nanofiber with a diameter of 100 nm has a specific surface area of 1000 m^2 g^{-1} [113]. Porous matrices developed using polymeric nanofibers have excellent structural and mechanical properties, high axial strength combined with extreme flexibility, high surface to volume ratio, high porosity (>70%), and variable pore sizes – all of these properties are highly beneficial for cell adhesion, migration and proliferation.

1.5.1.1 Top-down Approaches in Developing Scaffolds for Nano-based Tissue Engineering

The top-down approach is considered as a classical approach used to size down macrostructures to smaller sizes using various fabrication techniques. Several top-down techniques have been developed to form polymeric nanofibers from preformed macromolecules such as electrospinning, phase separation and templating [112, 114, 115].

Polymeric Nanofibers by Electrospinning Electrospinning has developed into a promising, versatile and economical technique to produce nanostructured scaffolds for tissue engineering [112, 116]. Figure 1.16 shows the schematic of the electrospinning process. Briefly in an electrospinning process an electric field is applied to a pendant droplet of polymer solution at the tip of a needle or capillary attached to a syringe or pipette. The polymer solution feed to the needle/capillary is controlled using a syringe pump or allowed to flow under gravity. The electrode can be either inserted in the polymer solution or connected to the tip of the needle. When an electric potential is applied to the droplet, the droplet will be subjected to couple of mutually opposing forces. One set of forces (surface tension and viscoelastic forces) tend to retain the hemispherical shape of the droplet and another set

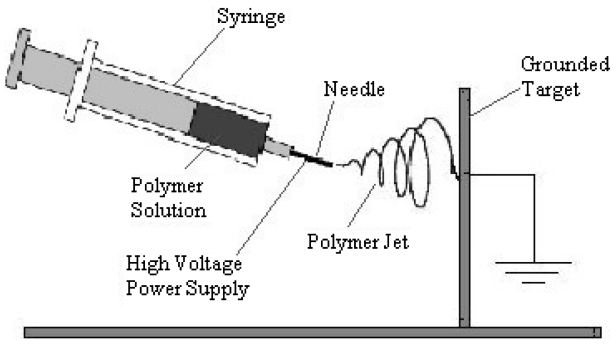

Fig. 1.16. Scheme of the electrospinning process.

of forces (due to the applied electric field) tend to deform the droplet to form a conical shaped ''Taylor cone''. Beyond a threshold voltage, the electric forces in the droplet predominate and at that point a narrow charged polymer jet will be ejected from the tip of the Taylor cone. However, the viscosity of the polymer solution plays a crucial role in maintaining the ejected jet. If the viscosity of the polymer solution is low, the ejected jet break into droplets by a process called ''electrospraying''. For solutions with higher viscosities, the ejected jet travels in a nearly straight line towards the grounded collector for some time due to the stabilization imparted by the longitudinal stress of the external electrical field on the charge carried by the jet. However, at some point along the course, the jet reaches a point of instability due to the repulsive forces arising from the opposite charges in the jet. The unstable jet then passes through a series of bending instabilities and it tends to bend back and forth following a bending, winding, spiraling and looping path in three dimensions. This bending instability of the jet has been demonstrated using high speed videography. During this process the polymer jet is continuously stretched resulting in significant reduction of the fiber diameter. This, along with the rapid evaporation of the solvent from the ultrathin jets results in the formation of ultrathin fibers that are deposited on a grounded collector surface [117–122].

Extensive studies have been performed to investigate the fundamental aspects of the process of electrospinning to determine the parameters that modulate the morphology and diameter of the electrospun fibers and for determining appropriate conditions for developing fibers from a wide range of polymers [112, 123–126]. These studies have clearly demonstrated the flexibility of the electrospinning process. Electrospun nanofiber scaffolds can be developed from a wide range of polymers with varying physical, chemical, and mechanical properties, thereby creating scaffolds with varying strength, surface chemistry, degradation patterns (in the case of matrix developed from bioresorbable polymers) and physical properties. The electrospinning process also enables co-spinning two or three different polymers, which further extends the ability to control the properties of the resulting scaffolds/matrices. Another advantage of electrospinning process is the feasibility of developing composite nanofiber scaffolds/matrices by incorporating small insoluble particles such as drugs or bioactive particles within polymeric nanofibers. Since the shape of the nanofiber scaffold/matrix depends on the properties of the collector, complex and seamless 3D structures can be developed using the appropriate collectors.

Parameters that Affect the Electrospinning Process Extensive studies have been undertaken to determine the parameters/variables that affect the electrospinning process. These include system parameters, solution properties and processing variables. The system parameters include the nature (chemistry and structure) of the polymer, molecular weight of the polymer and molecular weight distribution of the polymer. Solution properties include viscosity, elasticity, conductivity and surface tension of the polymer solution. The processing variables in the electrospinning process are electric potential, flow rate of the polymer solution, concentration of the polymer solution, the distance between the tip and the target,

ambient parameters such as solution temperature, humidity, air velocity in the electrospinning chamber, and motion of the target screen [112, 124, 126].

Most studies correlated the electrospinning parameters/variables to fiber diameter and/morphology. The effect of molecular weight of polymer on the process of electrospinning was evaluated using poly(ethylene oxide)s (PEO) of different molecular weights electrospun under identical conditions and by following the morphology of the fibers [127]. Figure 1.17(A–C) shows the effect of polymer molecular weight on the morphology of resultant nanofibers. In this study viscosity, surface tension and conductivity of all the solutions were kept constant to correlate the morphology of fibers to the molecular weight. Electrospinning of the low molecular weight polymer (20 000) resulted in the formation of mostly beads rather than fibers (Fig. 1.17A). Increasing the molecular weight to 500 000 resulted in the formation of fibers, however, with spindle shaped defect structures or beads (Fig. 1.17B). A further increase in molecular weight to 4×10^6 resulted in the formation of bead-free fibers (Fig. 1.17C). The formation of bead-free structures with high molecular weight PEO has been attributed to the increasing entanglement of the polymer chains with high molecular weight polymer.

The effect of electric potential and polymer concentration on the morphology and diameter of electrospun polymer fibers were demonstrated by Katti et al. using a bioresorbable polymer poly(lactide-*co*-glycolide) (PLAGA) [128]. PLAGA dissolved in a dimethyl formamide–tetrahydrofuran (1:3) mixture was used for electrospinning. The study demonstrated that the concentration of the polymer solution has a significant effect on the diameter and morphology of the electrospun fibers. Figure 1.18(A–C) shows the morphologies of PLAGA fibers formed from polymer solutions having different concentrations. A lower polymer concentration (0.15 g mL^{-1}) resulted in the formation of beaded nanofibers (Fig. 1.18A). Increasing the polymer concentration (0.2 g mL^{-1}) significantly reduced the probability of bead formation (Fig. 1.18B). The concentration also showed significant effects on the diameter of the resulting fibers. At low concentration (0.15 g mL^{-1}), fibers having diameters ~270 nm with beads were formed and increasing the concentration to 0.2 g mL^{-1} increased the diameter of the fibers to ~340 nm with minimal amount of beads. A further increase in concentration to 0.25 g mL^{-1} resulted in the formation of fibers having diameters ~1000 nm with apparently no bead formation (Fig. 1.18C). Increase in fiber diameter with increasing solution concentration followed a power law relationship. The same behavior has been observed for different polymer systems by other investigators [123, 129]. Demir et al., using polyurethane solution, have shown that fiber diameter can be correlated to polymer concentration as proportional to the cube of the polymer concentration [130].

Similarly the electrospinning voltage has a profound effect on the morphology and diameter of the fibers. An increase in electric voltage decreases the diameter of electrospun fibers up to a certain voltage and above that tends to increase the fiber diameter [126, 128]. Spinning voltage has been found to strongly correlate with the formation of beads. Deitzel et al. have shown that an increase in electrical potential increases the feasibility of formation of beads along the fibers [131].

In addition to varying the polymer concentration and the electric potential the

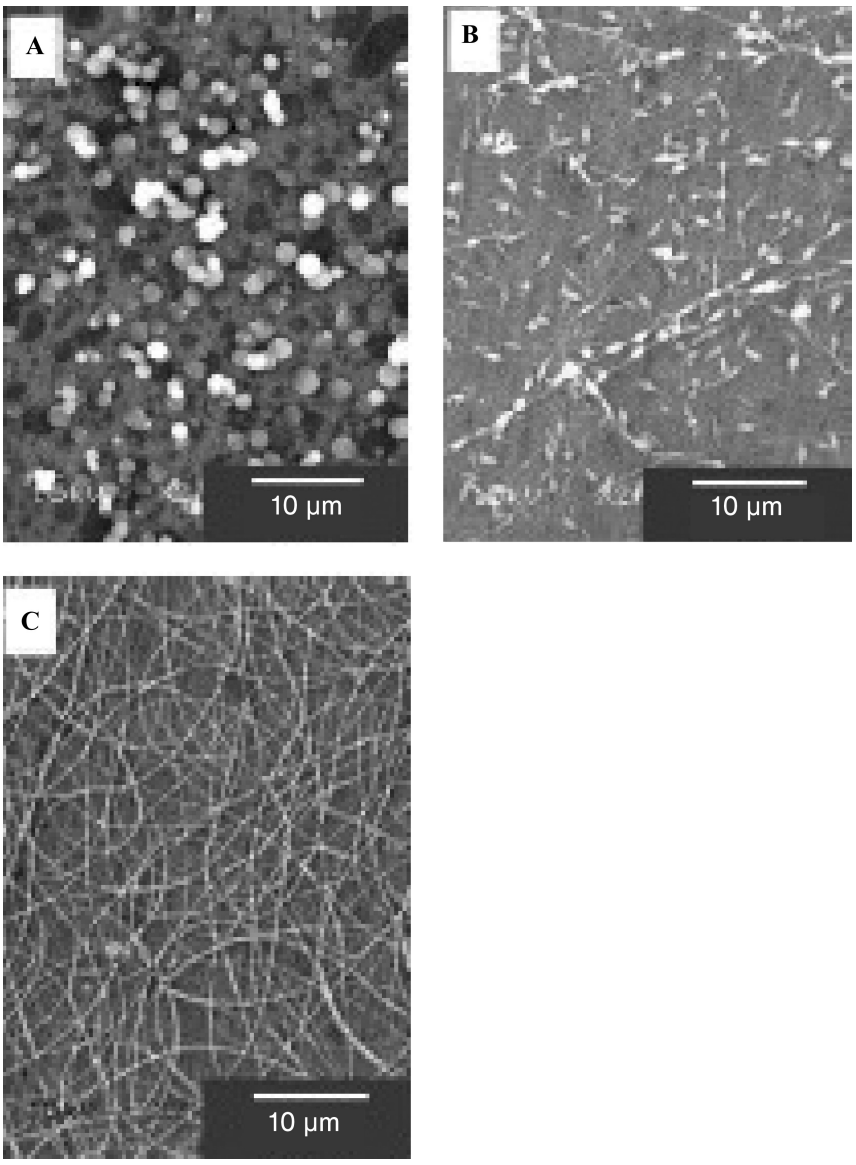

Fig. 1.17. Morphology of fibers formed by the electrospinning process using poly(ethylene oxide)s of different molecular weights: (A) 20 000, (B) 500 000, and (C) 4×10^6. (Adapted from Ref. [127] with permission from Elsevier.)

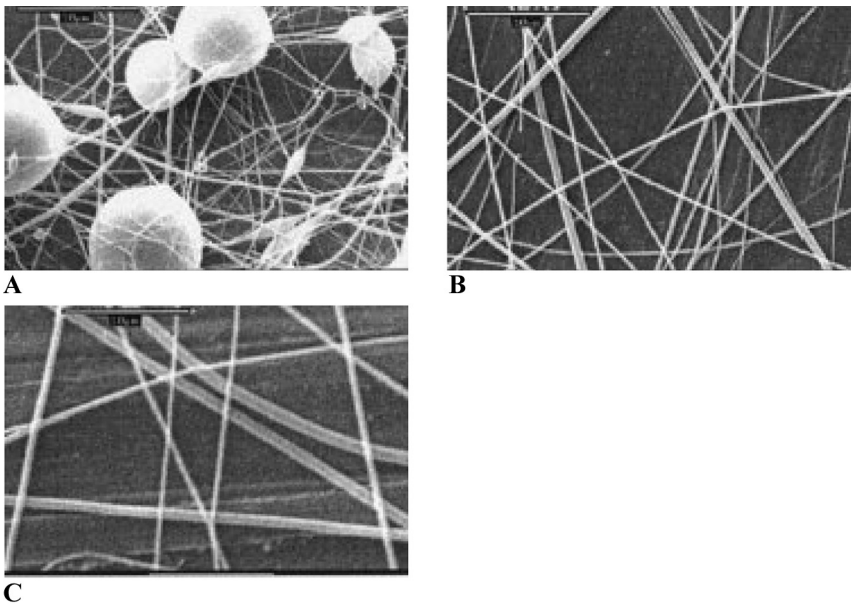

Fig. 1.18. Morphology of fibers formed by the electrospinning of PLAGA solutions having varying polymer concentrations (g mL^{-1}): (A) 0.15, (B) 0.2, and (C) 0.25. (Adapted from Ref. [128].)

diameter and morphology of electrospun polymer nanofibers can be modulated by the addition of various additives to the spinning solution. One study by Zong et al. has shown that addition of ionic salts to the polymer solution can significantly reduce the bead formation and could result in thinner fibers. This has been attributed to the higher charge density of the jet due to the presence of ionic salts. The higher the charge carried by the jet, the greater will be the pull or elongation force the jet will experience under the electrical field, resulting in fewer beads and thinner fiber [132].

The electrospinning process can also result in the formation of fibers having various cross-sectional features in addition to circular fibers, as demonstrated in the case of various polymers. Fibers having varying shapes have been created such as flat ribbon, bent ribbon, ribbons with other shapes, branched fibers and fibers that were split longitudinally from larger fibers from different polymers and polymer–solvent systems [133]. Figure 1.19 shows the SEM of fibers having varying cross-sectional shapes. The occurrence of skin on the polymer jet accounts for a number of these observations. The phenomenon has been attributed to various causes, including contribution of fluid mechanical effects, electrical charge carried by the jet, and evaporation of solvent from the jet. In addition to varied cross-sectional features, fibers have been found to form with surfaces having varying nanotopographies such as nanopores or ridges. The formation of these structures

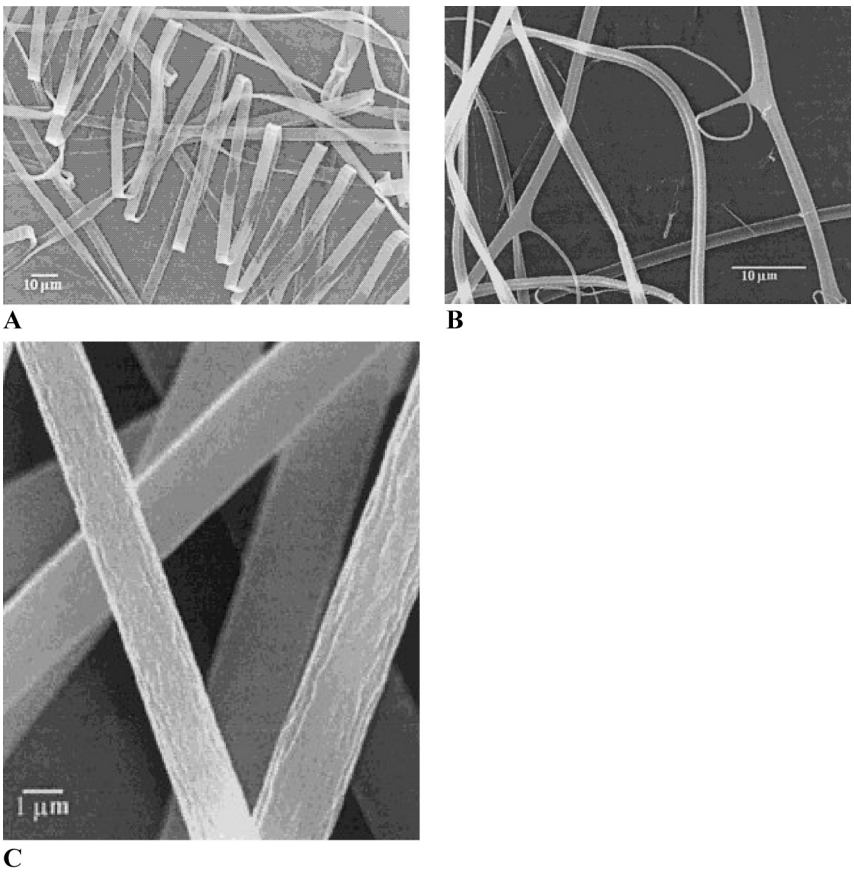

Fig. 1.19. SEM showing the fibers having varying cross-sectional shapes. (A) Flat ribbon formed from 10% solution of poly(ether imide). (B) Branched fibers from 16% HEMA. (C) Round fibers with skin collapsed to form longitudinal wringles. (Adapted from Ref. [133].)

have been attributed to various parameters such as the nature of the solvent, glass transition temperature of the polymer, solvent–polymer interactions, and environmental parameters such as humidity and temperature [134–136].

Nanofibers deposited by electrospinning using a static target result in the formation of a non-woven matrix composed of randomly oriented fibers. However, properties of fiber matrices can evidently be improved, if the fibers could be aligned in appropriate directions. This is particularly important for developing scaffolds for tissue regeneration as this would enable the development of scaffolds with specific orientation and architecture. Aligning the fibers formed by the process of electrospinning, however, is very difficult to achieve because during electrospinning process the jet trajectory follows a complex 3D whipping and bending path towards

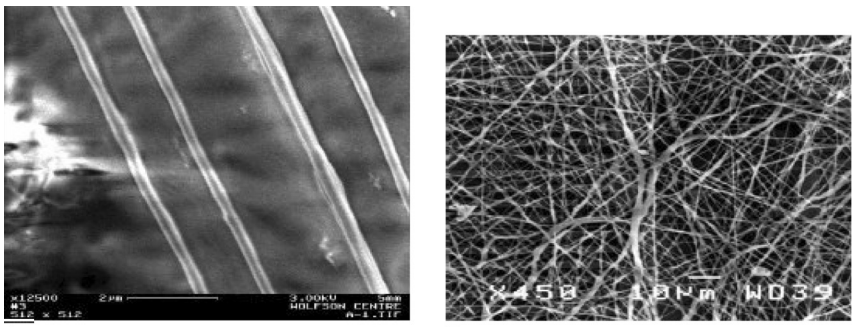

Fig. 1.20. SEM showing PEO nanofibers: (A) Aligned fibers and (B) randomly deposited fibers. (Reprinted from Ref. [139] with permission from Institute of Physics Publishing.)

the target rather than a straight line. Several attempts have been performed to develop aligned electrospun polymeric nanofibers. Earlier attempts were performed using a high speed rotating cylinder collector [137]. However, fiber alignment could be achieved only to a certain extent using this process, presumably due to the low control that can be achieved over a polymer jet that undergoes chaotic motion. In another attempt, an auxiliary electrical field was applied to align the fibers which substantially improved the fiber alignment [138]. Another successful approach to align electrospun nanofibers was developed by Theron et al. using a thin wheel with sharp edge device. The thin edge of the wheel helped to concentrate the electrical field so that almost all of the spun nanofibers were attracted and wound to the bobbin edge of the rotating wheel [139]. Figure 1.20(A and B) shows the SEMs of aligned PEO nanofibers developed using the thin wheel with sharp edge collector and randomly deposited fiber matrix using conventional static collector. Another approach investigated is the use of a frame collector and has been found to significantly improve the alignment of nanofibers [140]. In this process, however, the extent of alignment depends significantly on the frame material. Figure 1.21 shows the SEM of aligned PLLA-CL copolymer fibers formed by the frame method.

In addition to the above techniques, several processing techniques were also attempted to increase the versatility of the electrospinning process. These include electrospinning the mixture of polymer with sol–gel solution [141], electrospinning blend polymer solutions [142], electrospinning polymer solution containing nanomaterials to form composite matrices [126], core–shell nanofiber spinning [143] and side by side/multijet electrospinning of different polymers (to increase the rate of fiber deposition and develop matrices having unique properties such as biohybrid matrices) [144–146].

The electrospinning process is a very mild fabrication process. This makes it very attractive for developing structures for biomedical applications. Studies have shown the ability of electrospun fibers to preserve the biological activity of highly sensitive biomolecules encapsulated within the fibers during the electrospinning

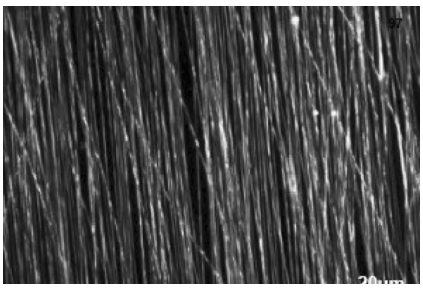

Fig. 1.21. Aligned PLLA-CL nanofibers formed by the frame method. (Adapted from Ref. [140] with permission from Elsevier.)

process. Hamdan et al. have encapsulated RNase and trypsin in poly(2-ethyl-2-oxazoline) nanofibers by electrospinning [147]. The enzymes were found to preserve their biological activity after being encapsulated within the nanofibers. Another study by Jiang et al. demonstrated the feasibility of incorporating model proteins such as bovine serum albumin and lysozyme within PCL nanofibers with preservation of their biological activity [148]. A novel electrospinning fabrication process called coaxial spinning was recently developed to encapsulate water-soluble macromolecules within hydrophobic nanofibers [143]. The fibers developed are called core–shell nanofibers where the aqueous phase containing the protein solution forms the core of the fiber surrounded by the hydrophobic polymer layer. The thickness of the core and the shell can be adjusted by the feed rate of the inner dope. Circular dichroism and SDS-PAGE studies on the released lysozyme and BSA encapsulated in the core–shell fibers revealed that both the proteins maintained their structure and bioactivity after encapsulation. The core–shell structures could have several advantages, such as improved protection of the encapsulated molecules and feasibility of achieving their controlled delivery when used as a macromolecular delivery vehicle for biomedical applications, including tissue engineering.

The mechanical properties of non-woven nanofiber matrices developed from bioresorbable polymers have been investigated. Thus, nanofiber matrices developed from PLAGA with LA:GA ratio of 85:15 showed a tensile strength similar to that of natural skin [149]. Ding et al. have demonstrated that the mechanical properties of non-woven nanofiber matrices could be further modulated by developing blend nanofibrous matrices using multi-jet electrospinning [144]. Another study by He et al. has demonstrated the low stiffness of non-woven polymeric nanofiber matrices compared to large diameter dacron grafts using poly(L-lactic acid-*co*-caprolactone) copolymer (PLLA-CL) nanofiber matrices. The low stiffness of the matrix makes it a suitable candidate for vascular graft applications [150]. The nanofiber matrix developed from PLLA-CL showed an ultimate strain of $175 \pm 49\%$. This high distension property has been attributed to the ability of the randomly oriented fibers to rearrange themselves in the direction of the stress. Another study compared the mechanical properties of nanofiber matrices with microfiber matrices developed

from poly(L-lactide-*co*-caprolactone) [PLCL] by the electrospinning process [151]. Three matrices composed of fibers with diameters of ~0.3, ~1.2, and ~7 μm were investigated. The differences in fiber diameter could lead to differences in specific density of the resultant matrices. The matrix composed of the smallest diameter fibers (~0.3 μm) gave the densest matrix. Also, the Young's modulus of the densest matrix (~0.3 μm) was the highest followed by the matrix composed of fibers having diameter 1.2 μm. The matrix composed of fibers with diameter ~7 μm showed the lowest Young's modulus. This indicates that nanofiber matrices could show better mechanical performance than microfibrous matrices of the same material presumably due to the increase in fiber density. In terms of the mechanical properties of aligned nanofiber matrices developed by electrospinning, the nanofiber matrices showed different properties along different directions [152]. The ultimate strength of the aligned polyurethane fiber matrices (3520 ± 30 kPa) was significantly higher than randomly deposited fiber matrices (1130 ± 21 kPa) [153].

In summary, these studies demonstrate the feasibility of developing polymeric nanofibers with diameters ranging from 1 to 1000 μm from a wide range of polymers using the process of electrospinning. The diameter and morphology of the nanofibers can be controlled to a great extent by varying the process parameters/variables that govern the electrospinning process. The properties of the matrices fabricated using polymeric nanofibers can be modulated by varying the properties of the polymer, co-spinning or multiple spinning polymer mixtures, incorporating nanoparticles or fillers, varying the rate of deposition as well as varying the properties of the target. The feasibility of aligning the fibers significantly increases the ability to modulate the properties of nanofiber matrices for biomedical applications. Another notable advantage of the electrospinning process is the cost effectiveness compared to other nanofabrication techniques.

Polymeric Nanofibers by Phase Separation Phase separation is another type of top-down approach used to develop polymeric nanofiber matrices from different polymer solutions. This technique has been found to be effective in developing nanofibrous matrices having high porosities (up to 98.5%) from biodegradable polymers and has been investigated for tissue engineering applications [154].

Liquid–liquid phase separation can be achieved by lowering the temperature of a polymer solution having an upper critical solution temperature. The phase separation at low temperature could lead to the formation of a continuous polymer-rich and polymer-lean solvent phases. The removal of solvent from the phase separated system at low temperature affords a scaffold with an open porous structure [154, 155]. Thus the development of nanofibrous porous matrices using phase separation of polymer solution takes place in five steps. Polymer dissolution in a solvent system, phase separation and gelation, solvent extraction from the gel with water, freezing and freeze drying under vacuum [114]. Similar to the electrospinning process, various processing variables can be controlled to modulate the properties of the nanofibrous matrices formed by phase separation process. These include type of solvent and polymer, polymer concentration, solvent exchange, thermal treatment and order of procedures [114].

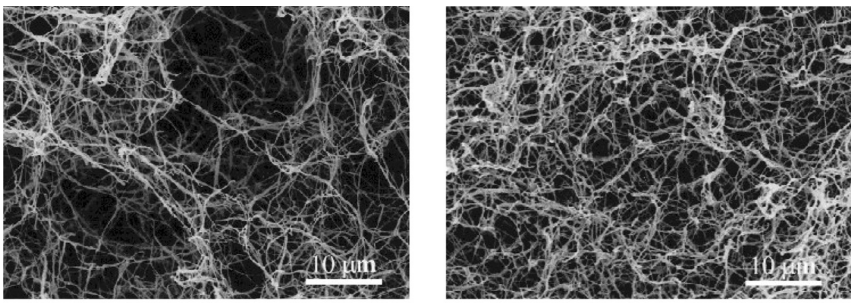

Fig. 1.22. SEM micrographs of PLLA fibrous matrices prepared from PLLA/THF solution with different PLLA concentrations at a gelation temperature of 8 °C: (A) 1% and (B) 5% (w/v). (Adapted from Ref. [154].)

Ma and Zhang have developed 3D continuous nanofibrous structures that could mimic the structure of the ECM using biodegradable poly(L-lactic acid) [PLLA]. Fibers of the nanofiber matrix exhibited diameters in the range 50–500 nm. Figure 1.22(A and B) shows the SEM of PLLA fibrous matrices prepared from 1% (w/v) and 5% (w/v) PLLA/THF solution. The figures demonstrate the feasibility of varying the porosity of matrices by varying the concentration of the polymer solution. The higher the concentration of the solution, the lower was the porosity of the matrices formed.

Another advantage of fabricating nanofibrous matrices using the phase separation technique is that it allows for incorporation of macropores along with nanopores in the matrices by adding various porogens such as sugars, inorganic salts or paraffin spheres to the mold with the polymer solution during phase separation [156]. Figure 1.23(A and B) shows macro-nano porous matrices of PLLA fabricated by the combined porogen leaching phase separation method. Thus the phase separation process is a mild processing technique that provides the flexibility to control the properties of the nanofiber matrices such as fiber diameter, interconnectivity, porosity and size of the pores.

1.5.1.2 Bottom-up Approaches in Developing Scaffolds for Nano-based Tissue Engineering

Bottom-up approaches are based on self-assembly, a ubiquitous natural phenomenon that harnesses the physical and chemical forces operating at the nanoscale to assemble small building blocks into larger structures. Thus, the basic principle of the bottom-up approach is molecular self-assembly, which is the spontaneous organization of molecules under near thermodynamic equilibrium conditions into structurally well-defined and stable arrangements through non-covalent interactions [157]. These interactions include weak non-covalent bonds, such as hydrogen bonds, ionic bonds, hydrophobic interactions, van der Waals interactions and water-mediated hydrogen bonds [158]. The development of a self-assembling sys-

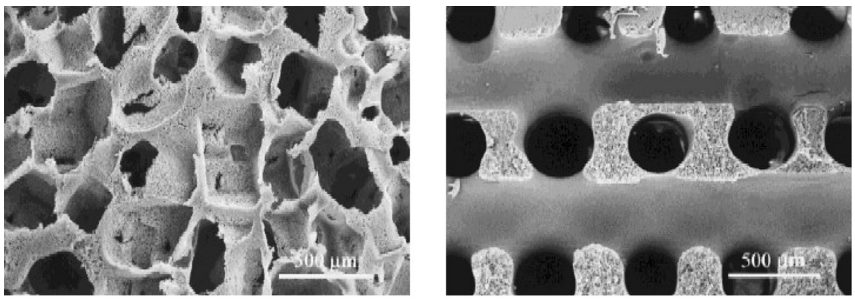

Fig. 1.23. (A) SEM micrograph of PLLA nano-fibrous matrix with particulate macropores prepared from PLLA/THF solution and sugar particles; particle size 250–500 mm. (B) SEM micrograph of PLLA nano-fibrous matrix with an orthogonal tubular macropore network prepared from PLLA/THF solution and an orthogonal sugar fiber assembly. (Adapted from Ref. [156].)

tem requires the design and development of small building blocks that can spontaneously self-assemble and be stabilized to form functional nano/microstructures. Recently, there has been significant interest in using self-assembly to develop nanostructured scaffolds for tissue engineering.

The most extensively investigated self-assembled nanostructured scaffolds for tissue engineering application are developed from peptide molecules. In 1993, Zhang et al. demonstrated the feasibility of an aqueous solution of a 16-residue ionic self-complementary peptide to spontaneously associate to form a macroscopic membrane [159]. The ionic complementary oligopeptides used in the study have regular repeating units of positively charged residues (lysine or arginine) and negatively charged residues (aspartate or glutamate) separated by hydrophobic residues (alanine or leucine). The membrane was highly stable to varying pHs and temperatures [159]. SEM of the self-assembled membrane revealed that the structure is composed of nanofibers with diameters ranging from 10 to 15 nm. The study raised interest in self-assembling peptide motifs and led to the development of different self-assembling peptide structures capable of assembling into unique nanostructures. Thus different types of self-assembling peptides have been identified to form different self-assembled structures such as nanofibers, nanotubes, nanowires and nanocoatings. Among these the Type I peptides also called molecular Legos developed by Zhang et al. have been identified as a potential peptide motif for developing self-assembled scaffolds for tissue engineering. These peptide motifs are called molecular Legos because at the nanometer scale they resemble the Lego bricks that have pegs and legs in a precisely determined organization. These peptides form β-sheet structures in aqueous solution resulting in distinct hydrophilic and hydrophobic surfaces [158–160]. The hydrophobic surface shields the peptide motif from water, thereby enabling them to self-assemble as in the case of protein folding *in vivo*. Then complementary ionic bonds will be formed with regular repeats on the hydrophilic surface. The complementary ionic sides have been

classified into different moduli based on the chemistry of the hydrophilic surface, i.e., having alternating positive and negative charged amino acid residues with different intervals. Depending on the moduli, these molecules could under go ordered self-assembly to form nanofibers. These nanofibers, due to their high aspect ratio, in turn associate to form nanofiber scaffolds that closely mimic the porosity and gross structure of the ECM, making them potential candidates as tissue engineering scaffolds [161]. Figure 1.24(A) illustrates the formation of nanofibrous structures using molecular Lego. ''PuraMatrix'' a commercially developed ECM mimic self-assembling molecular Lego system has been found to be suitable for performing 3D tissue culture *in vitro*. The nanofiber scaffolds formed from these peptide motifs are formed of interwoven nanofibers with diameter of ~10 nm and pores of ~5–500 nm with very high water content (>99.5%) (Fig. 1.24B).

Naturally occurring amino acids were used in developing peptide motifs in these studies. However, studies by Stupp et al. demonstrated the feasibility of using building blocks other than natural amino acids to create amphiphilic peptides. The peptide amphiphiles were developed from appropriate amino acids using solid phase peptide chemistry and the NH terminus of the peptide sequence was then alkylated to form the amphiphilic molecule. The amphiphilic peptides (PA) molecules are composed of a peptide segment containing 6–12 amino acids coupled via an amide bond to a fatty acid chain that varies in length from 10 to 22 carbon atoms. Even at very low concentrations of 0.25% (w/v) these molecules can self-assemble to form a gel structure composed of a network of cylindrical nanofibers with diameter ranging from 5 to 8 nm, depending on the length of the self-assembling molecules. The matrices were highly hydrated (>99.5%) and the mechanical integrity of such a highly hydrated matrix has been attributed to the high aspect ratio of the nanofibers composing the matrix. These molecules are custom developed so that they can self-assemble to form nanostructured scaffolds that could structurally and biologically mimic the structure of the ECM of specific tissue type. Thus, a composite nanostructured matrix has been developed as potential scaffolds for bone tissue engineering. The scaffold was designed to mimic the ECM of natural bone by self-assembling peptide motifs with appropriate amino acids and mineralizing the matrix *in vitro* [162]. In this study the peptide amphiphile was designed as follows. To make robust nanofibers four consecutive cysteine amino acids were incorporated in the sequence. The cysteine residues were incorporated as they could form disulfide linkages between adjacent molecules upon oxidation to stabilize the supramolecular structure. The formation of the disulfide linkage, however, is a reversible process. A phosphoserine residue was incorporated into the peptide sequence, so that after self-assembly the resulting fibers will have highly phosphorylated surface. These groups are specifically incorporated in the PA to increase the mineralizing capacity (nucleation and deposition of hydroxyapatite an essential inorganic component of natural bone) of the nanostructured scaffold. Anionic groups are known to promote nucleation and deposition of hydroxyapatite on synthetic materials and phosphorylated groups are particularly important in the formation of calcium phosphate minerals. Thus, the phosphorylated surface of self-assembled nanofibers could promote the nucleation and deposition

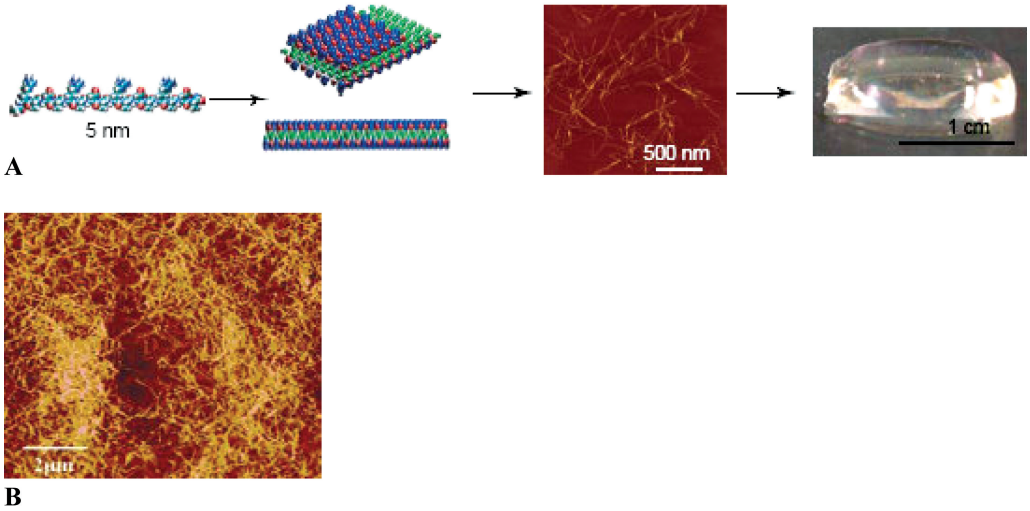

Fig. 1.24. Fabrication of various peptide materials. (A) Peptide Lego, also called ionic self-complementary peptide, has 16 amino acids, ~5 nm in size, with an alternating polar and nonpolar pattern. The peptide motifs could form stable β-strand and β-sheet structures. The peptide motifs undergo self-assembly to form nanofibers with the nonpolar residues inside (green) and positive (blue) and negative (red) charged residues forming complementary ionic interactions, like a checkerboard. These nanofibers form interwoven matrices that produce a scaffold hydrogel with very high water content (~99.5%). (Adapted from Ref. [161] with permission from Elsevier.) (B) AFM image of the nanofiber scaffold (PuraMatrix). (Adapted from Ref. [161] with permission from Elsevier.)

of hydroxyapatite (HA). To improve the cell adhesivity of the self-assembled nanofiber matrix, an RGD sequence was also incorporated in the peptide. Figure 1.25 shows the structure of the PA molecule designed to self-assemble to form nanofiber scaffold for bone tissue engineering.

The nanofiber scaffold was developed from the PA as follows. The cysteine residues of the PA were first reduced to thiol groups at higher pH. The resulting PA was found to be highly soluble in water. The pH of the aqueous solution was then reduced to 4.0, at that point the material rapidly became insoluble due to the formation of network structure. Cryo-transmission electron microscopy (Cryo-TEM) showed that the gel is composed of a network of fibers that are 7.6 ± 1 nm in diameter and up to several micrometers long. Figure 1.26(A and B) shows the ultrastructure of the gels formed by self-assembly with and without covalent stabilization. The ability of the nanofiber matrix formed from the PA to nucleate hydroxyapatite (HA) along the fiber axis was also demonstrated by incubating the nanofiber matrix in appropriate salt solution (Fig. 1.26C). Another interesting property of the self-assembled gel is its reversibility. The self-assembled matrix could disassemble at higher pHs. Even though the study demonstrated for the first time the feasibility of designing and developing bioactive self-assembled system to mimic the properties of the ECM, it has certain disadvantages. The significant

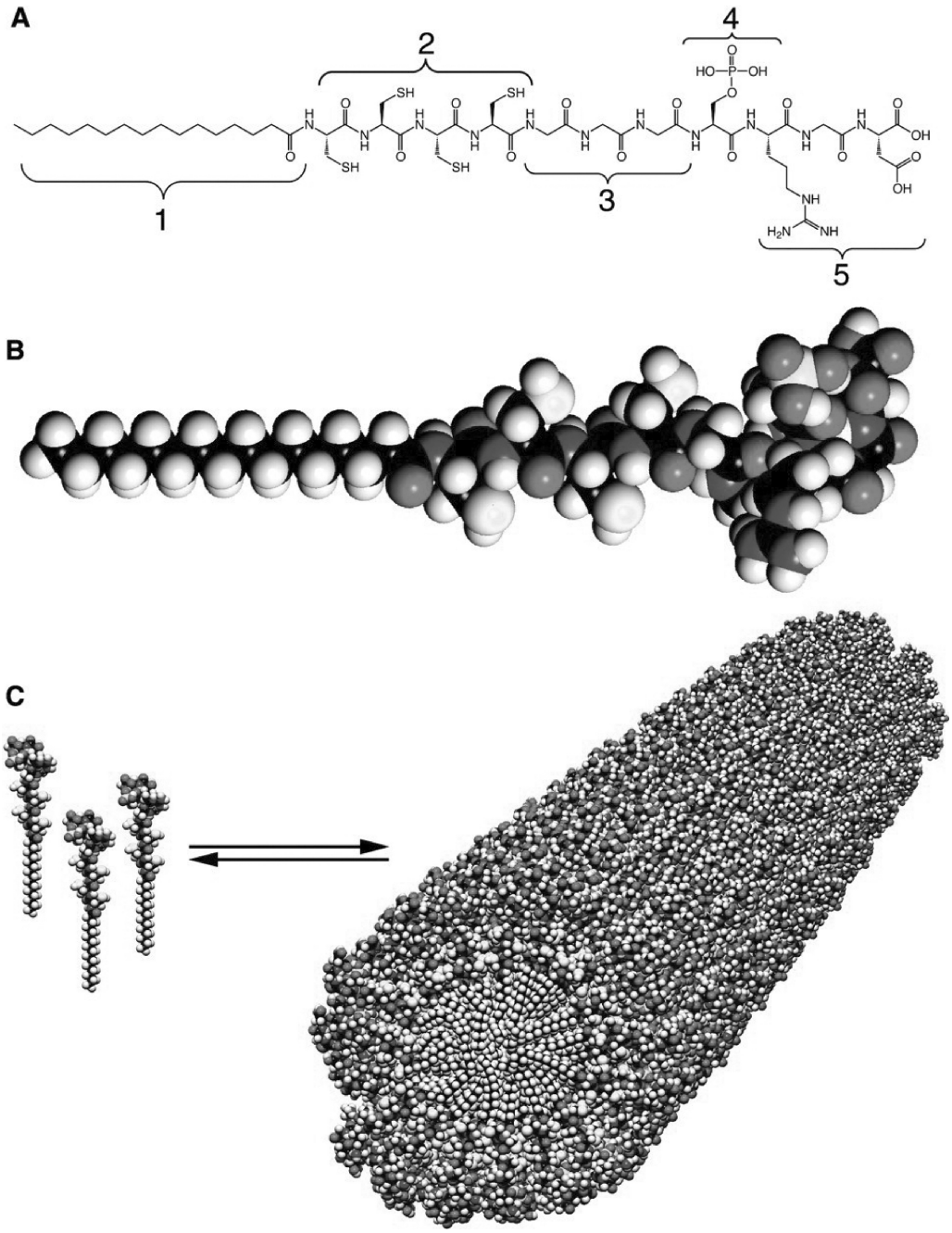

Fig. 1.25. (A) Chemical structure of the peptide amphiphile. Region 1 is a long alkyl tail to make the peptide motif amphiphilic. Region 2 is composed of four consecutive cysteine resides for disulfide linkages. Region 3, a flexible linker region of three glycine residues, provides hydrophilic head group flexibility from the rigid crosslinked region. Region 4 is a single phosphorylated serine residue. Region 5 is a cell adhesion RGD ligand. (B) Molecular model of PA. (C) Scheme showing the self-assembly. (Reprinted with permission from Ref. [162].)

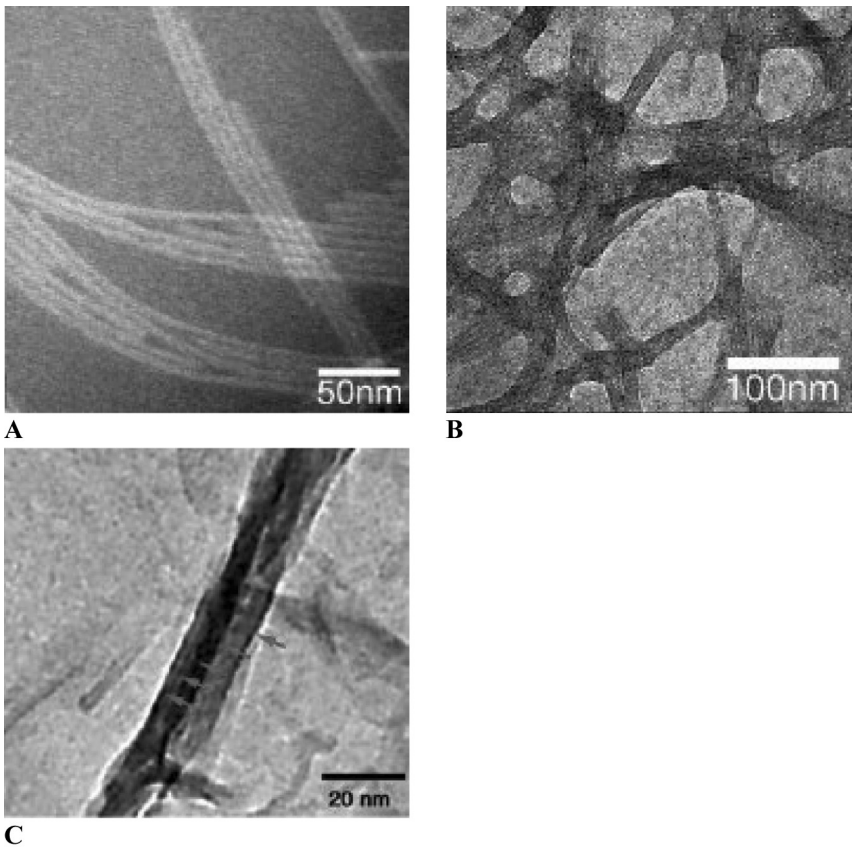

Fig. 1.26. TEM of self-assembled nanofibers (A) before and (B) after covalent stabilization. (C) TEM showing PA nanofibers completely covered by mature hydroxyapatite crystals. (Reprinted with permission from Ref. [162].)

disadvantage of this system is the low stability of the self-assembled structure at physiological pH unless internally crosslinked by covalent bonds. Another study was therefore performed to demonstrate the feasibility of developing self-assembled structures that are stable at physiological pH using PAs with opposite charges based on the electrostatic attraction of the opposite charge [163]. Mixed systems having oppositely charged PAs were used to develop self-assembled systems capable of assembling at physiological pH due to electrostatic attraction. This ability of these materials to undergo mild self-assembly and gelation at physiological conditions and the ability to decorate them with bioactive motifs makes them potential candidates for various biomedical applications.

In addition to peptide motifs, synthetic proteins were also investigated to develop self-assembled matrices. Thus Petka et al. used a recombinant DNA method to cre-

ate artificial proteins that can undergo reversible gelation in response to pH or temperature. The developed proteins consist of terminal leucine zipper domains flanking a central flexible water-soluble polyelectrolyte segment [164]. In near neutral solution, a 3D network can be formed by coiled-coil aggregates of the terminal domains and the polyelectrolyte segment prevent precipitation of the chain and retain the solvent. An elevation of pH or temperature leads to dissolution of the gel, resulting in the formation of viscous polymer solution. Similarly Nowak et al. developed a diblock copolypeptide amphiphile containing charged and hydrophobic segments, which were found to form hydrogels with high temperature stability [165]. The ability of this system to form gel under mild conditions makes them potential candidates for biomedical applications.

Both top-down and bottom-up approaches have significantly contributed to the development of nanostructured matrices as scaffolds for tissue engineering. The top-down approaches currently used to develop nanofiber matrices such as electrospinning or phase separation are highly economical and easily scalable processes. Furthermore, nanofiber scaffolds with finely controlled physical and mechanical properties and complex structures can be developed due to the versatility of the fabrication processes. The bottom-up approach even though is a more involved process that requires highly specific building blocks for spontaneous self-assembly has several advantages from a biomaterials point of view. The matrix formation via a mild self-assembling process makes it a very attractive process for *in vivo* applications. Another advantage is the ease of incorporating specific bioactive motifs as the building blocks that when combined with the nanostructured topography of the resulting matrix could better mimic the structure and functions of the extracellular matrix. The major disadvantage of the self-assembly process, however, is its relative inability to generate complex patterns for biological devices due to its homogeneous character.

1.6
Cell Behavior Towards Nano-based Matrices

Several studies have confirmed the fact that cells prefer to live in a complex nanostructured environment composed of pores, ridges and fibers of the polymeric nanofiber matrices that mimics the structure of the ECM compared to 2D matrices or microfiber matrices. Kwon et al. have evaluated the adhesion and proliferation potential of human umbilical vein endothelial cells (HUVEC) on three different types of PLL-CL fiber matrices composed of fibers having diameters ~0.3, ~1.2, and 7 μm [151]. Figure 1.27 shows the SEMs of HUVECs cultured for 1 and 7 days on electrospun matrices having fibers of different diameters (0.3, 1.2, and 7 μm). The matrix composed of the smallest diameter fibers (0.3 μm) and the medium diameter fibers (1.2 μm) showed higher cell adhesion and proliferation than matrix composed of fibers having diameter 7 μm. The morphology of the cells on 0.3 and 1.2 μm fiber matrices were comparable but differed significantly from that on the matrix composed of 7 μm diameter nanofibers. Thus the matrices com-

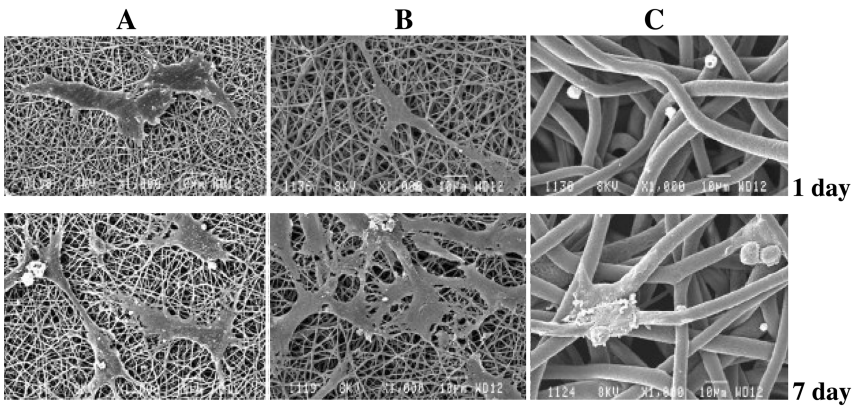

Fig. 1.27. SEM showing the morphologies of HUVECs cultured for 1 and 7 days on PLCL (50/50) electro-spun fibers having different diameters (μm): (A) 0.3, (B) 1.2, and (C) 7. (Adapted from Ref. [151] with permission from Elsevier.)

posed of 0.3 and 1.2 μm diameter fibers promoted the adhesion, spreading and proliferation of cells and the cells were found to be anchored on many fibers on the surface of the matrices. The quantitative determination of cell adhesion on these two matrices did not show any statistically significant differences in cell proliferation. However, the cells on the 7 μm fiber matrix were found to be rounded and showed significant decrease in cell proliferation compared to the other two matrices. This low cell adhesion and proliferation on microfiber matrix has been attributed to the large interfiber distance or a very low surface density of fibers that could not permit cell adhesion between the neighboring fibers.

Schindler et al. have investigated the ability of nanofibrillar matrix to promote *in vivo*-like organization and morphogenesis of cells in culture [166]. The synthetic nanofibrillar matrices were prepared by electrospinning a polymer solution of polyamide onto glass cover slips. The matrices were found to be composed of fibers of diameters ∼180 nm and a pore diameter of ∼700 nm. The surface smoothness of the matrix was found to be within 5 nm over a length of 1.5 μm, which is similar to the 3D organization of fibers in the basement membranes. NIH 3T3 fibroblasts, normal rat kidney (NRK) cells and breast epithelial cells were used for the *in vitro* evaluation. The organizational and structural changes of the intracellular components (actin and focal adhesion components) of the cells were measured as a function of adhesion when cultured on nanofibrous matrices and compared with the responses to cells on glass substrate. Fibroblasts plated on the glass substrate were well spread with an elaborate checkerboard pattern of stress fibers (Fig. 1.28A). Cells on the nanofiber matrix, however, showed significant changes in the morphology and shape. Compared to cells on the glass substrates, the cells on the nanofiber matrices were more elongated and bipolar with thinner actin fibers arranged parallel to the long axis of the cell. Notable increases in the formation of actin-rich lamellipodia, membrane ruffles and cortical actin were also observed

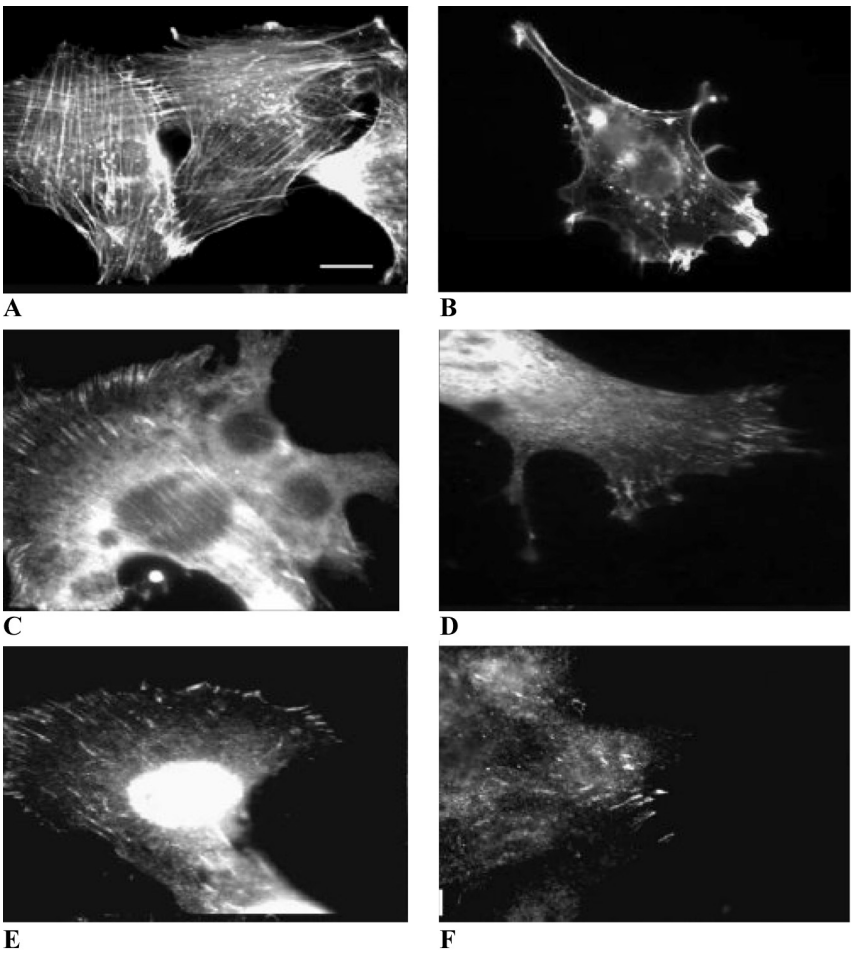

Fig. 1.28. Comparison of the F-actin network, focal adhesion components, fibronectin organization and integrin antibodies for NIH 3T3 fibroblasts cultured on glass substrates and nanofiber matrices. (A, C, E, G, I) are cells on glass substrates and (B, D, F, H and J) are cells on nanofiber matrices (see text for details). (Adapted from Ref. [166] with permission from Elsevier.)

(Fig. 1.28B). Staining of vinculin (a prominent component of focal complexes and focal adhesions that links cytoskeleton, plasma membrane and the ECM) of fibroblasts cultured on glass substrate showed a parallel streaked structure (Fig. 1.28C). However, the streaked staining for vinculin within cells on nanostructured matrix was limited to the edge of the lamellipodia with a more diffuse staining throughout the cell cytoplasm (Fig. 1.28D). Similar to actin distribution, such pattern of vinculin labeling correlates with cellular differentiation and morphogenesis *in vivo*. The cells were also stained for focal adhesion kinase (FAK) which functions as a central mechano-sensing transducer in cells. Cells cultured on glass demon-

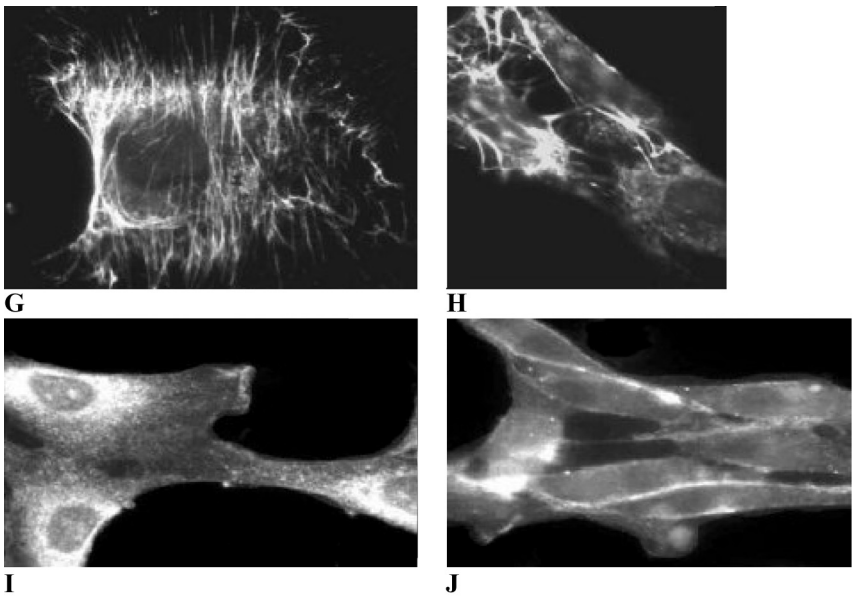

Fig. 1.28 (*continued*)

strated a streaky pattern of FAK labeling similar to the pattern obtained for vinculin (Fig. 1.28E). However, for cells on nanofiber matrix, the localization of FAK was found to be more punctuated and less well defined (Fig. 1.28F). Previous studies using breast epithelial cells have correlated this loss of FAK localization at focal adhesions to morphogenesis and differentiation [167]. The distribution of fibronectin on the cell surface cultured on glass substrate for 24 h revealed a classic linear pattern of fibrils (Fig. 1.28G). The cells on the nanofiber matrix, however, showed a thicker network of more randomly deposited apically localized fibrils indicating that they are permissive for the assembly of a matrix that can promote the formation of 3D-matrix adhesions (Fig. 1.28H). Staining for β1 integrin for NPK cells was punctuated when cultured on glass substrate for 24 h (Fig. 1.28I). However, the cells on nanofibrous matrix showed an organized long slender aggregate staining pattern, indicating the localization of β1 integrin in focal adhesions (Fig. 1.28J).

The ability of nanofiber matrices to promote morphogenesis was demonstrated by culturing T47D epithelial cells on glass and nanofiber coated glass matrices [166]. The T47D cells were used in the present study as they have been demonstrated to form duct like tubular structures and spheroids under conditions that promote morphogenesis. After 5 days in culture, a mixed population of multicellular structures comprised of tubules and spheroids were found on nanofiber matrix. At day 10, multicellular spheroids were dominant compared to tubules. Figure 1.29(A) shows a confocal series through a multicellular spheroid showing a lumen formed on nanofiber matrix. The figure shows the ability of T47D cells to grow into a complex multilayer structure on a nanofiber matrix. The cells cultured on

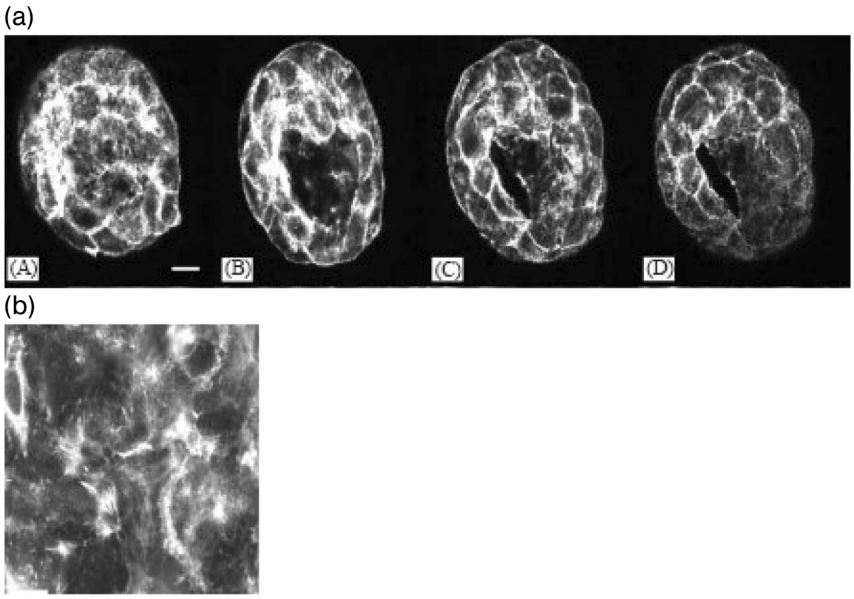

Fig. 1.29. (a) A series of confocal sections of a multicellular spheroid composed of T47D breast epithelial cells grown on nanofibers and stained with phalloidin-Alexa Fluor (A–D). (b) Cells after 10 days of culture on glass substrate. (Adapted from Ref. [166] with permission from Elsevier.)

glass surface, in contrast, formed a monolayer with groups of F-actin fibers (Fig. 1.29B). These studies demonstrated the advantages of using nanofiber matrices compared to microfiber matrices or 2D surfaces in developing 3D tissues, demonstrating their potential as ideal scaffolds for tissue engineering application.

1.7 Applications of Nano-based Matrices as Scaffolds for Tissue Engineering

Due to the unique properties and favorable cell behavior towards nanofiber matrices, different nanofiber matrices developed by top-down and by bottom-up approaches have been investigated as potential scaffolds for developing various tissues. The following section overviews nanofiber-based matrices as scaffolds for tissue regeneration.

1.7.1 Stem Cell Adhesion and Differentiation

As stem cells have been identified as one of the most appropriate cells for tissue engineering, the interaction of nanofiber matrices with stem cells raise significant

interest. The unique ability of nanofiber matrices to support the growth and differentiation of stem cells into appropriate lineages have been demonstrated using self-assembled protein nanofiber matrices. Silva et al. have demonstrated the feasibility of encapsulating neural progenitor cells (NPCs) in self-assembled bioactive peptide amphiphiles and the ability of the cells to differentiate to appropriate lineage [168]. NPCs were selected as they are extensively used to replace lost central nervous system cells after degenerative or traumatic insults. Owing to the design flexibility of peptide amphiphiles as described earlier, unique PA was developed for form self-assembled scaffolds that could provide favorable environment for NPCs. The peptide motif designed to develop the scaffold was composed of a pentapeptide epitope isoleucine-lysine-valine-alanine-valine (IKVAV). The epitope has been selected because it is present in laminin, a cell adhesive protein present in the ECM and known to promote neurite sprouting and direct neurite growth. In addition to the neurite sprouting epitope, a GLu residue was also incorporated in the peptide that could give the peptide a net negative charge at pH 7.4. The rest of the molecule is composed of four Ala and three Gly followed by an alkyl tail of 16 carbon atoms.

The peptide was soluble in aqueous media and upon addition of cell suspension the cations present in the cell culture media screened the electrostatic repulsion, allowing the molecules to self-assemble due to hydrogen bond formation. Upon self-assembly the bioactive motifs were found to be placed on the surface. Figure 1.30 shows the SEM of nanofiber matrix formed by the self-assembly of peptide amphiphiles. A control amphiphile was also developed with a non-physiological sequence of glutamic acid-glutamine-serine (EQS) to compare the cell response to the bioactive self-assembling PA. Even though the control matrices allowed the encapsulation of the progenitor cells by self-assembly, the encapsulated cells did not sprout neuritis or differentiate morphologically or histologically.

The NPCs encapsulated within the peptide amphiphile self-assembled matrix was found to be viable throughout the period of study of 22 days. No differences in cell viability between the encapsulated cells and cells cultured on polylysine 2D

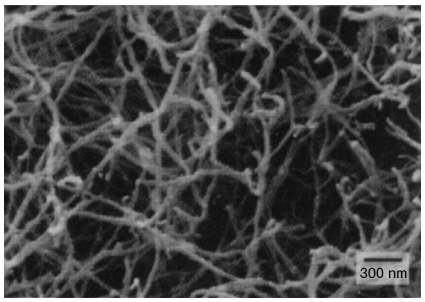

Fig. 1.30. SEM showing the morphology of scaffold developed from an IKVAV nanofiber network by adding cell culture media to the peptide amphiphile. The sample is dehydrated and critical point dried caged in a metal grid to prevent network collapse during sample preparation for SEM. (Reprinted with permission from Ref. [168].)

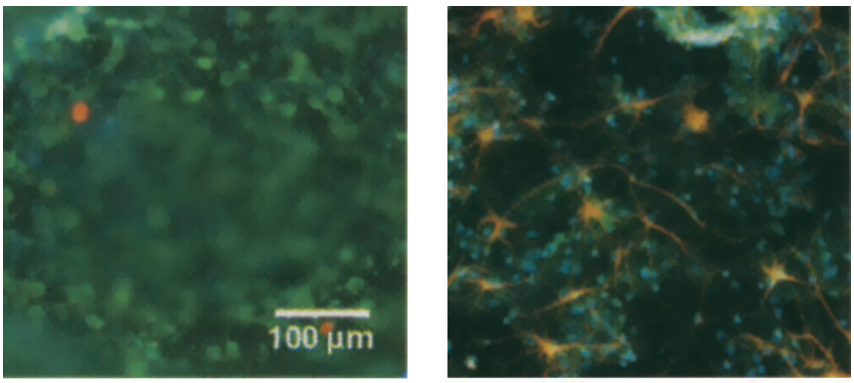

Fig. 1.31. Immunohistochemistry showing β-tubulin III of neurons and astrocytes of cells encapsulated in self-assembled bioactive gels (A) (after 1 day in culture) and lamine-coated cover slips (B) (after 7 days in culture). β-Tubulin III is stained green, differentiated astrocytes (glial cells) are labeled orange. (Reprinted with permission from Ref. [168].)

films were found demonstrating that sufficient diffusion of nutrients, bioactive factors and oxygen is taking place through the highly hydrated nanofiber matrix. Immunocytochemistry demonstrated the differentiation of NPCs encapsulated in the bioactive self-assembled PA matrix to neurons. Furthermore, the results were found to be statistically significant when compared to cells grown on laminin or lysine coated surface. Differentiated neurons were labeled for β-tubulin III and glial fibrillary acidic protein to detect neurons and astrocytes. After only 1 day in culture, 35% of the cells encapsulated within the bioactive nanofiber scaffold stain positive for β-tubulin (Fig. 1.31A). At the same time only less than 5% of the cells in the bioactive scaffold showed astrocyte differentiation even after 7 days in culture (Fig. 1.31A). This is a positive observation since inhibition of astrocyte proliferation is important in the prevention of the glial scar a known barrier to axon elongation following CNS trauma. Cells cultured on 2D laminine coated substrate did not show such differentiation and at the same time showed significant astrocyte proliferation (Fig. 1.31B). Encapsulation in the nanofiber scaffold led to the formation of large neurites after only 1 day (57 ± 26 µm) where as cells grown on laminin or lysine did not form neurites at that time. TEM evaluation of cells encapsulated within the gels after 7 day showed a healthy and normal ultrastructural morphology. The high migrating ability of the cells encapsulated within the gels was also demonstrated by tracking the distance between the center of each neurosphere and cell bodies as a function of time. The study demonstrated the potential of bioactive self-assembling nanofiber scaffolds as stem cell delivery vehicles.

The differentiation ability of progenitor cells into different lineages on polymeric nanofiber matrices developed by electrospinning was demonstrated recently by Li et al., using multipotent human mesenchymal stem cells (MSC). The study demonstrated the feasibility of nanofiber matrices to support the adhesion and differen-

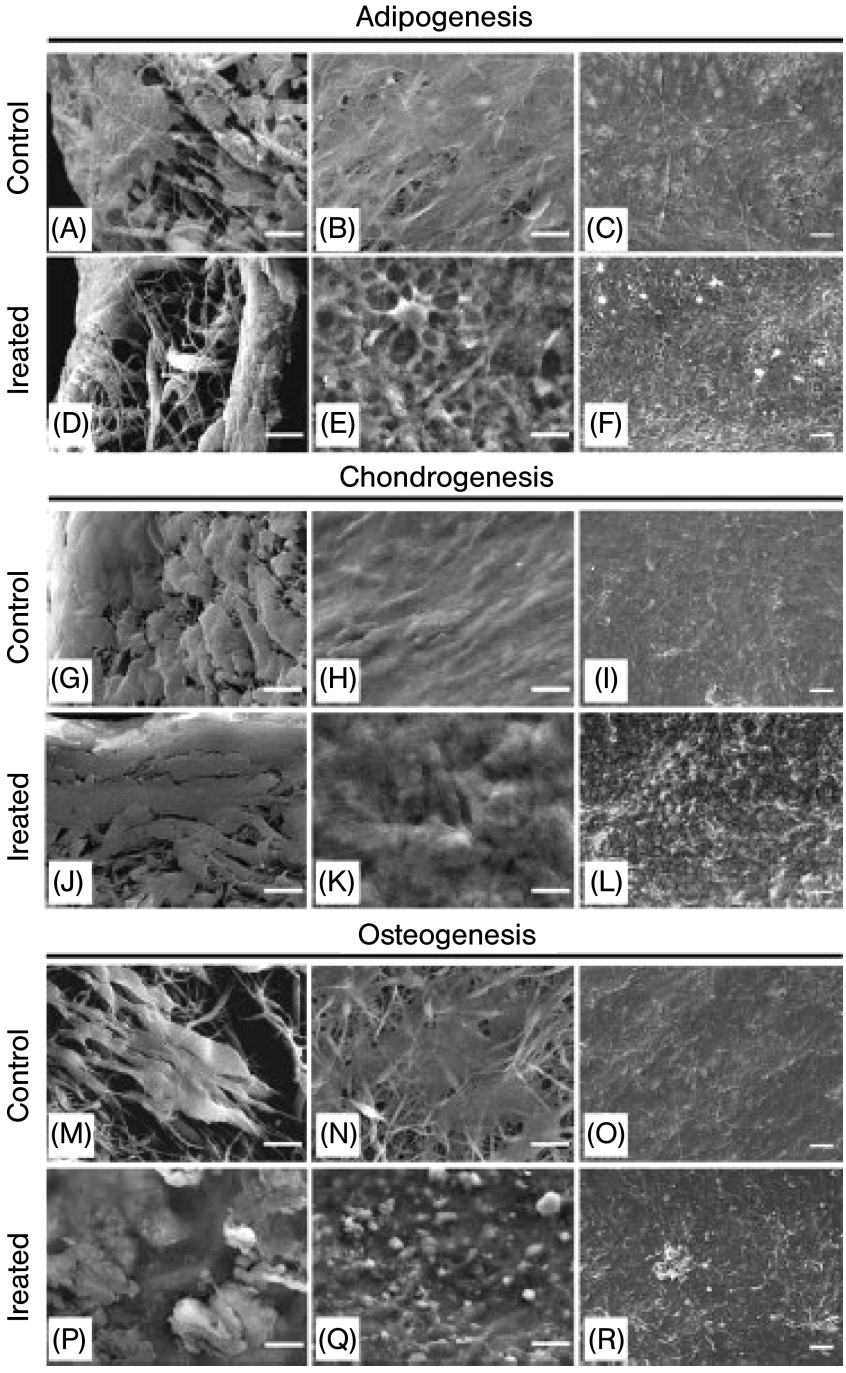
Adipogenesis
Control
Ireated
(A)
(B)
(C)
(D)
(E)
(F)
Chondrogenesis
Control
Ireated
(G)
(H)
(I)
(J)
(K)
(L)
Osteogenesis
Control
Ireated
(M)
(N)
(O)
(P)
(Q)
(R)

tiation of these cells into different lineages [169]. PCL nanofiber matrices were used for the study. The matrix was found to be composed of randomly oriented nanofibers having diameters ~700 nm. The MSCs seeded on the nanofiber matrices were found to attach and remained viable. For multi-lineage differentiation of the cells the MSC seeded nanofiber matrices where placed under specific differentiation promoting culture conditions (Fig. 1.32). Thus, under adipogenic conditions (media with dexamethazone, 3-isobutyl-1-methylxanthine and insulin), the cell–polymer constructs developed into an adipose like tissue with the cells expressing appropriate gene expression. The incubation of the cell seeded nanofiber matrices in chondrogenic media resulted in the formation of a cartilaginous tissue composed of cells showing characteristic chondrocyte phenotypes. The authors observed that the chondrogenic differentiation of MSC on nanofiber matrices takes place even at low cell population compared to 2D cultures or cells encapsulated in hydrogels presumably due to the unique interactions of the cells with the nanostructured topography of the matrix. Incubation of the cell seeded nanofiber matrix in osteogenic media (β-glycerophosphate, ascorbic acid and dexamethasone) resulted in the formation of a dense bone-like tissue with the cells showing characteristic osteoblast phenotypes. The study thus demonstrated that electrospun nanofiber scaffolds can support chondrogenic, osteogenic and adipogenic differentiation and, therefore, are candidate scaffolds for the fabrication of multi-component tissue constructs.

1.7.2 Neural Tissue Engineering

Nerve tissue engineering can be considered as one of the most promising approaches to restore central nervous system function. Several studies have evaluated the efficacy of nanofibrous matrices as scaffolds for neural tissue engineering. In one study Yang et al. determined the efficacy of PLLA nanofiber matrices developed by phase separation process as scaffold for neutral tissue regeneration [170]. The fiber diameters were ~196 nm with a matrix porosity of ~85%. Neural stem cells (NSC) were used in the study. Upon NSC seeding and culturing for a day, the cells were found to randomly spread over the surface of the polymer scaffold without much differentiation. By day 2 the cells had progressively grown throughout the scaffold, with a neurite length twice that of the cell body, and migration of cells

Fig. 1.32. SEM showing nanofiber–MSC constructs maintained with and without differentiation media (A–F adipogenic; G–L chondrogenic; and M–R osteogenic). (A, D, G, J, M, P) Cross sections; (B, C, E, F, H, I, K, L, N, O, Q, R) top views. In adipogenic cultures (D–F), globular, round cells were evident, while fibroblast-like cells were found in the control cultures (A–C). In chondrogenic cultures (J–L), round chondrocyte-like cells were embedded in a thick layer of ECM that was not found in the control group (G–I). In osteogenic cultures (P–R), mineralized nodules were formed in the constructs. In contrast, control cultures (M–O) contained primarily fibroblast-like cells, and mineralization was not seen [169] with permission from Elsevier.

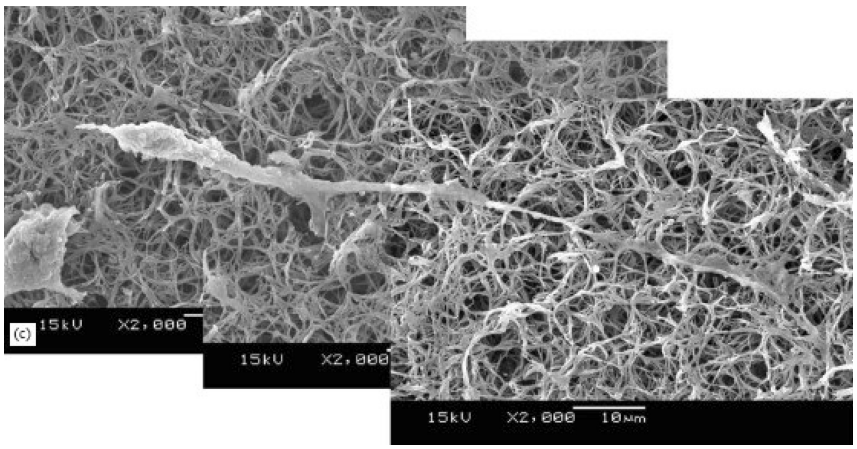

Fig. 1.33. SEM showing the magnified view of a differentiated cell with long neurite cultured on a nanofiber matrix developed by phase separation. (Adapted from Ref. [170] with permission from Elsevier.)

into the porous matrix also occurred (Fig. 1.33). The study showed the feasibility of nanofibrous scaffold to act as a positive guidance cue to guide neurite outgrowth.

Efficacy of aligned polymeric nanofiber matrices as a scaffold for the growth and differentiation of neural NSCs was further evaluated by Yang et al. using PLLA nano/microscaffold [171]. The cell adhesion and differentiation pattern on the aligned nanofiber matrices were compared to aligned microfiber matrices formed by electrospinning as well as random micro and nanofiber matrices. The aligned nanofiber matrices were composed of fibers having diameter ~300 nm and microfiber matrices were composed of fibers having diameter ~1.5 μm. The average fiber diameters of the random nano and microfiber matrices were ~250 nm and 1.25 μm respectively. NSC attached and formed an elongated spindle-like shape on all the surfaces. The direction of NSC elongation and neurite outgrowth was found to be aligned with the direction of aligned fibers and showed classical contact guidance. The cells on random fiber matrices in contrast showed significantly different phenotype. In terms of differentiation, more cells were found to be differentiated on aligned nanofiber matrix (80%) than on aligned microfiber matrix (40%) demonstrating that nanofiber alignment has profound effect on cell differentiation. Since successful nerve regeneration rely on the extensive growth of axonal process, the neurite length of cells on the matrices was evaluated. The neurite length of NSCs on aligned nanofiber matrix was significantly higher than aligned micromatrix or random matrices. Figure 1.34 shows the SEM micrograph of NSC on aligned nanofiber matrix. The cells body shows an apparent bipolar elongated morphology with the outgrowing neuritis. Both cell elongation and neurite outgrowth followed the same direction of PLLA nanofibers. The figure also shows significant interaction between NSCs and the aligned fibers. Some filament-like

Fig. 1.34. SEM showing the interaction of NSC on an aligned PLLA nanofiber matrix. Bar = 5 μm. (Adapted from Ref. [171] with permission from Elsevier.)

structures, presumably focal adhesions, extend out from the NSC cell body and neurite and attach to the nanofiber. This study thus demonstrated that aligned nanofiber matrix could improve NSC differentiation and support neurite outgrowth compared to other matrices evaluated.

1.7.3 Cardiac and Blood Vessel Tissue Engineering

One of the major reasons for the failure of synthetic small diameter vascular grafts is adverse blood biomaterials interactions resulting in an acute occlusion followed by a chronic intimal hyperplasia. The ability to engineer vascular grafts using biodegradable scaffolds could lead to the development of synthetic grafts with long-term patency. One of the most extensively investigated approaches to prevent graft occlusion is to improve the antithrombogenicity of graft materials by seeding them with endothelial cells. But the development of a stable endothelial covering on the surface of synthetic materials is difficult due to the high sensitivity of the endothelial cells.

Mo et al. have evaluated the efficacy of polymeric nanofiber matrices as scaffolds for growing endothelical and smooth muscle cells [172]. P(LLA-CL) nanofiber

matrices developed by the process of electrospinning were used as the 3D scaffold in the study. Endothelial cells and smooth muscle cells were cultured on the nanofiber matrices for 7 days. Both SMC and EC adhered and spread on nanofiber matrices with the cell number, showing a significant increase from day 1 to day 7. This indicates the ability of the cell to attach and proliferate on the nanofiber matrix. Immunohistochemical evaluation of adhered ECs on the nanofiber matrix showed appropriate EC phenotype expression, indicating favorable interaction of the cells with the matrix.

Even though self-assembly of bioactive peptide motifs can be considered as the direct method to develop bioactive nanofiber matrices, He et al. have recently demonstrated the feasibility of improving the bioactivity of electrospun nanofibers by surface modification. They modified the surface of a P(LLA-CL)nanofiber matrix to improve the efficacy of the matrix towards endothelial cell attachment and proliferation [150]. The surface of p(LLA-CL) nanofiber matrix was functionalized by plasma modification and the nanofiber matrix surface was then coated with collagen. Human coronary artery endothelial cells (HCAECs) were used to evaluate the efficacy of the coated nanofiber scaffold compared to uncoated scaffold. The cells on uncoated scaffold were rounded in shape without significant spreading (Fig. 1.35A). More cells were found to be attached on the collagen-coated p(LLA-CL) nanofibers than uncoated nanofiber matrix since collagen is the main structural and functional protein present in ECM (Fig. 1.35B). Immunohistochemical evaluation of the cultured cells showed the preservation of endothelial phenotype by the cells on the coated nanofiber matrix.

Similarly a collagen coated PCL nanofiber matrix was evaluated for improve SMC adhesion and interaction [173]. Coating the nanofibers with collagen improved the cell adhesion on the fibers, with cells preserving their characteristic phenotype.

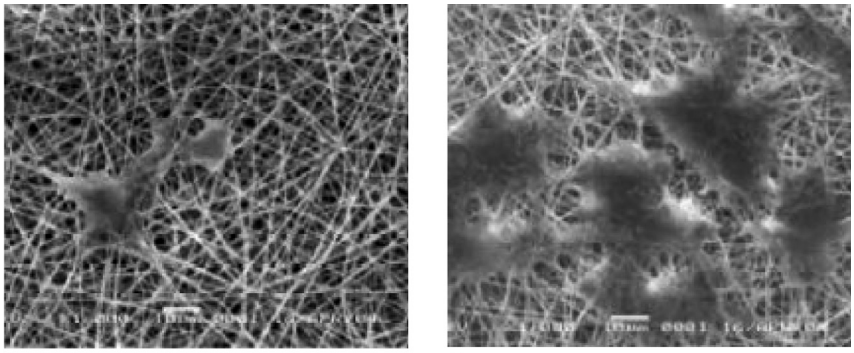

A **B**

Fig. 1.35. SEM images of HCAECs cultured on (A) uncoated P(LLA-CL) nanofiber matrix and (B) collagen-coated p(LLA-CL) nanofiber matrix after 3 days in culture. (Adapted from Ref. [150] with permission from Elsevier.)

Another related study was performed by the same research group to evaluate the effect of cell behavior towards scaffolds that combine nanostructure and bioactivity. Poly(ethylene terephthalate) a non-degradable polymer extensively investigated for developing vascular graft was fabricated into a nanofibrous structure using the process of electrospinning [174]. The nanofibers were then surface modified to attach a bioactive protein gelatin. The surface-modified fiber scaffolds were then seeded with HCAECs and cultured for 7 days. The surface-modified nanofiber matrix showed improved cell adhesion and maintenance of phenotypic activity. These results showed that combining the nanostructure of the scaffold with the bioactive molecule could positively promote cell–matrix and cell–cell interactions, inducing them to express the phenotypic shape.

The effect of fiber orientation on SMC attachment and proliferation of nanofiber matrices was evaluated using aligned nanofiber scaffolds of P(LLA-CL) [140]. Aligned fibers were developed by the process of electrospinning using the wheel with a sharp edge collector. SMCs were found to adhere on aligned nanofiber scaffold as early as within 1 h of seeding and the cells tend to elongate along the direction of the nanofibers. After 3 days in culture, SMCs proliferated approximately along the longitudinal direction of the nanofiber length, which formed an oriented pattern similar to those in native artery. The cell number significantly increased at day 7 and the surface of the nanofibrous scaffold was covered with a continuous SMC monolayer with a regular direction from left to right along the nanofiber alignment. The cell adhesion and proliferation on aligned nanofiber matrix was significantly higher than on 2D film of the same polymer. Figure 1.36 shows the SEM of aligned SMC on aligned nanofiber matrix. Further, the distribution and organization of cytoskeleton proteins inside SMCs were parallel to the direction of the nanofibers (Fig. 1.37). The study demonstrated for the first time the feasibility of using an aligned nanostructured scaffold to mimic natural vessel architecture and the ability of cells to orient along the fiber axis to mimic the natural orientation.

One elegant method to incorporate biofunctionality into nanofiber scaffolds is the use of self-assembling peptides decorated with appropriate protein motifs. Gen-

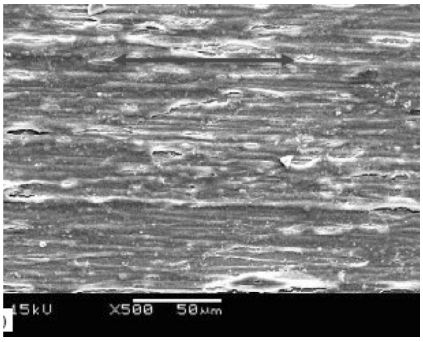

Fig. 1.36. SEM showing the alignment of SMCs along the aligned nanofiber matrix. (Adapted from Ref. [140] with permission from Elsevier.)

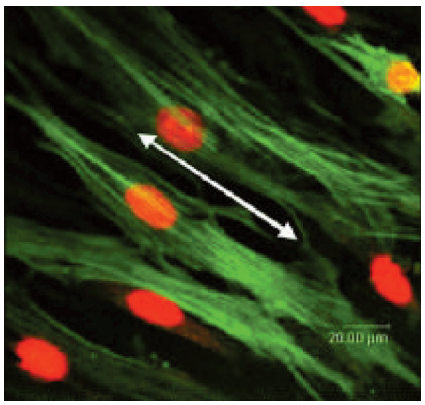

Fig. 1.37. LSCM micrograph of immunostained α-actin filaments in SMC after 1 day of culture on aligned nanofiber matrix. (Adapted from Ref. [140] with permission from Elsevier.)

ove et al. recently developed biomimetic self-assembled peptide scaffolds and evaluated the function of human aortic endothelial cells seeded on the scaffolds [175]. The self-assembling protein motifs were developed based on the functionality of basement membrane, which is composed mainly of laminin and collagen. Two peptide sequences present in laminin (YIGSR and RYVVLPR) are known to promote cell adhesion, cell migration and endothelial cell tubular formation, and a peptide sequence in collagen Type IV (TAGSCLRKFSTM) shown to promote the adhesion and spreading of bovine aortic endothelial cells, were selected to develop novel functionalized peptide motifs for self-assembly. The functionalized peptides were developed by solid-phase synthesis and found to self-assemble to form hydrogel under physiological conditions (Fig. 1.38). Four different scaffolds were investigated in the study, unmodified self-assembled peptide scaffolds, composed of RAD 16-1 (AcN-RADARADARADARADA-CONH2), YIG (10%) modified scaffold, RYV (10%) modified scaffold and TAH (10%) modified scaffold. Cell numbers increased about two-fold in modified peptide scaffolds compared to unmodified scaffolds, indicating that cell could sense and respond to the functionalized material. In addition, the matrix could modulate endothelial cell growth only when the sequence was physically attached to the nanofiber matrix, showing the importance of spatial distribution of the bioactive molecules on the nanostructured scaffolds. The peptide scaffolds in general also enhanced the endothelial cell phenotype, such as NO synthesis and deposition of basement membrane components (laminin I and collagen IV), suggesting the potential of these scaffolds in recreating the endothelial microenvironment.

Another application for which biodegradable nanofiber matrices have been evaluated is for developing scaffolds for engineering myocardium. Shin et al. have evaluated the potential of PCL nanofiber matrix as a cardiac graft by assessing the interaction of rat cardiomyocytes with the nanofiber scaffold [176]. The average di-

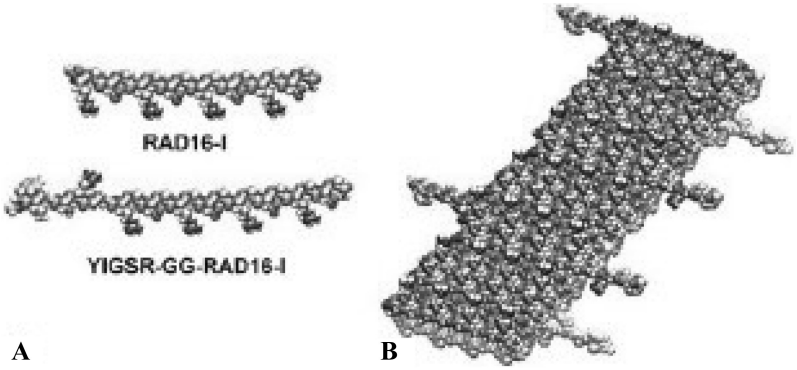

Fig. 1.38. (A) Model representing the peptide RAD16-1 (unfunctionalized peptide) and peptide YIG (functionalized). (B) Model representing the double β-sheet tape of a self-assembled peptide nanofiber of a mixture composed of RAD16-1 and YIG (9:1). (Adapted from Ref. [175] with permission from Elsevier.)

ameter of the fibers used to develop the scaffold was ~250 nm. The cardiomyocytes attached well on the scaffold and after three days in culture the cardiomyocytes started to contract (Fig. 1.39). The contractions were ubiquitous and synchronized. The mechanical property (softness) of the scaffold was found to be highly appropriate to allow the spontaneous contraction of the cardiomyocytes. The cardiomyocytes were also found to form a tight arrangement and intercellular contacts throughout the entire mesh and stained positive for cardiotypical proteins. However, the system has some limitations for *in vivo* application. The limited thickness of the scaffold might not be able to provide sufficient function when used alone to cover an infracted area. Therefore, a modified multilayered nanostructured nanofibrous graft was developed [177]. PCL nanofiber matrices composed of fibers having diameters of ~100 nm were developed and cardiomyocytes were cultured on nanofiber matrices for 5–7 days. After that layering of the individual grafts (five

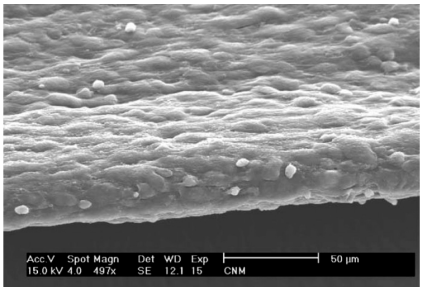

Fig. 1.39. SEM of the cross-section of a cardiac nanofibrous mesh, showing complete coverage of the mesh with cardiomyocytes. (Adapted from Ref. [176] with permission from Elsevier.)

layers) were performed by gently placing layers on top of each other. The layered constructs were incubated for 2 h at 37 °C without media for interlayer attachment and then cultured for 14 days in culture media. Multilayered scaffolds initially showed weak and unsynchronized contractions but became stronger and synchronized with time. H&E staining of the constructs demonstrated the interconnections between the layers. The immunohistochemistry study showed the presence of connexin43 in multilayered graft, indicating that the cells are rebuilding gap junctions, and synchronized contractions in multilayered grafts. *In vivo* studies using these grafts are under way.

1.7.4 Bone, Ligament and Cartilage Tissue Engineering

Nanofiber matrices were also investigated for developing scaffolds for bone, ligament and cartilage tissue engineering. Li et al. used PLAGA nanofiber matrices to culture MSCs and demonstrated that nanofibrous matrices could support the adhesion and proliferation of these cells [149]. Yoshimoto et al. used PCL nanofiber matrices to culture MSCs under dynamic conditions in osteogenic media to evaluate the feasibility of developing bone *in vitro* [178]. The average fiber diameter of the scaffold was ~400 nm. The MSCs were seeded on the nanofiber matrix and cultured for 4 weeks under dynamic conditions. MSCs were found to attach and proliferate throughout the nanofiber matrix. Furthermore, the cells migrated inside the scaffold and produced an extracellular matrix of collagen throughout the scaffold (Fig. 1.40). After 4 weeks in culture the cell polymer construct was noticeably harder and the extracellular matrix was calcified throughout the matrix, as evidenced from histology.

Polyurethane nanofiber scaffold was used to evaluate the effect of nanofiber alignment on the cellular response of human ligament fibroblasts (HLF) and to evaluate the influence of HLF alignment and strain direction on mechanotransduction [153]. A rotating collecting target was used to develop aligned nanofibers. After 3 days in culture, the HLFs on the aligned nanofibers were spindle shaped

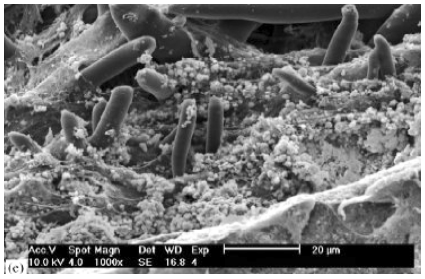

Fig. 1.40. SEM showing a cell nanofiber construct after 4 weeks in culture. Globular accretions, abundant calcification and collagen bundles can be seen. (Adapted from Ref. [178] with permission from Elsevier.)

and oriented (similar to *in vivo* ligament fibroblast morphology) along the nanofiber direction and the aligned nanofiber formed tissue-like oriented bundles that were confluent over the entire surface within 7 days. The HLFs on randomly oriented nanofiber scaffold were not oriented, but when the scaffold was subjected to uniaxial strain the cells reorganized their spindle shape and became organized. There were significant differences in the ECM production by oriented and unoriented cells on the matrices, indicating that cell morphology plays a significant role in ECM production. Furthermore, the aligned HLFs on the nanofiber structure were more sensitive to strain in a longitudinal direction. The study demonstrated that aligned nanofiber scaffold forms a promising structure for developing tissue engineered ligament due to its biomimetic structure and the ability to provide a mechanical environment ligament cells encounter *in vivo*.

Li et al. using PCL nanofiber scaffold demonstrated the efficacy of nanofiber scaffold to support the differentiation of MSCs to chondrocytes as a viable method to engineer cartilage *in vitro* [179]. The three-dimensional MSC seeded constructs display a cartilage-like morphology containing chondrocyte like cells surrounded by abundant cartilaginous matrix (Fig. 1.41). The level of MSC chondrogenesis using nanofiber scaffold was found be higher than in high density pellet cultures commonly used for MSCs. This study this demonstrated that biodegradable nanofiber scaffold due to its microstructure resemblance to a native ECM effectively supported MSC chondrogenesis.

A self-assembling peptide hydrogel scaffold has also been investigated as scaffolds for cartilage repair and regeneration [180]. A KLD12 peptide was developed, the aqueous solution of which was found to form a hydrogel when exposed to salt solution or cell culture media. The encapsulated chondrocytes showed a round morphology with cell viability of 89% immediately after encapsulation. Cell division of encapsulated chondrocytes in peptide hydrogel was found to be much higher than agarose control cultures. Histological evaluation of the encapsulated cell–hydrogel construct showed the formation of cartilage-like ECM rich in proteoglycans and type II collagen. Time dependent accumulation of this ECM was paralleled by increase in stiffness of the material showing the deposition of mechanically functional neo-tissue. This study demonstrated the potential of self-assembling peptide hydrogel as a scaffold for the synthesis and accumulation of a true cartilage-like ECM within a 3D cell culture for cartilage tissue repair.

1.8 Conclusions

Nanotechnology assisted fabrication processes are changing the way bioresorbable scaffolds are being developed for tissue engineering. Novel nanofabrication processes have enabled the development of nanostructured scaffolds that could closely resemble the structure of the ECM, and studies using bioactive nanostructured scaffolds have demonstrated the importance of nanostructure in cell–matrix and cell–cell interaction. Even though top-down and bottom-up approaches developed

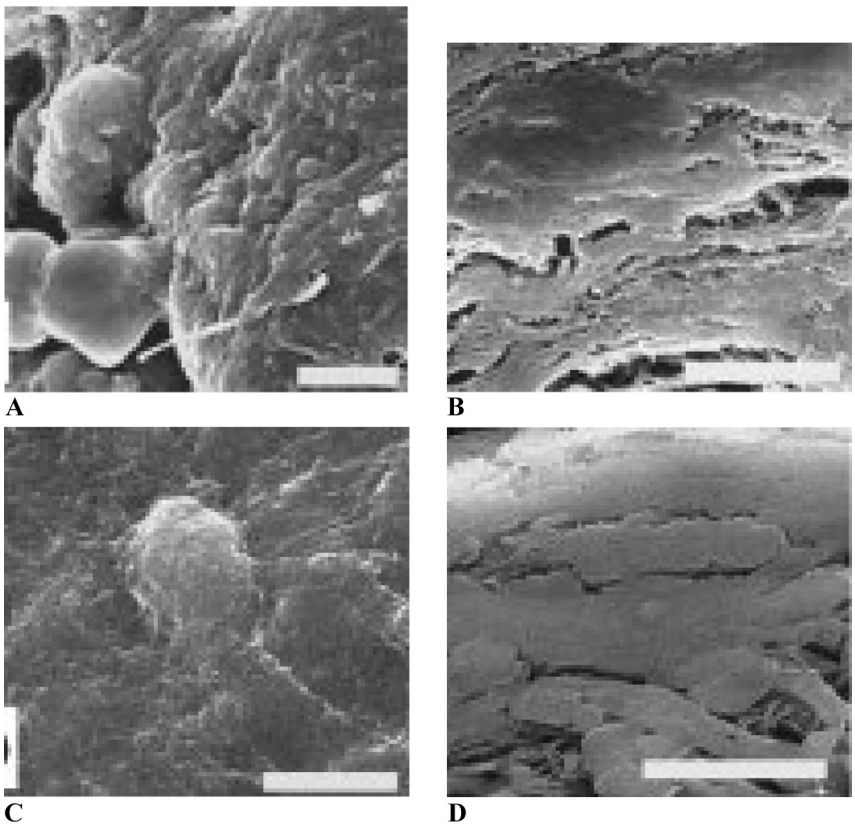

Fig. 1.41. Morphology of differentiated chondrocytes in cell pellet (CP) culture and using PCL nanofiber matrix. (A) Top view of CP with round chondrocyte-like cells on the surface. (B) Cross-sectional view of CP, showing thick ECM. (C) Top view of nanofiber matrix, showing the presence of round, ECM-embedded chondrocyte-like cells. (D) Cross-sectional view of nanofiber matrix, showing a thick, dense ECM-rich layer. (Adapted from Ref. 179] with permission from Elsevier.)

to fabricate nanostructured scaffolds have several advantages of their own, several limitations still hinder the translation of many of these technologies for clinical applications. Future studies will rely on a combination of both approaches as necessary as well as combining these with lithographic techniques to develop hierarchical nanostructures with spatially presented biological cues for developing optimal scaffolds for tissue engineering.

References

1 Levenberg S, Langer R. *Curr. Top. Develop. Biol.* 61, 113–134, **2004**.

2 Bauer TW, Muschler GF. Bone graft materials An overview of the basic

science. *Clin. Orthop.* 371, 10–27, **2000**.

3 Heineken FG, Skalak R. Tissue engineering: A brief overview. *J. Biomech. Eng.* 113, 111, **1991**.

4 Skalak R, Fox CF (eds.). *Tissue Engineering*, Proceedings for a Workshop held at Granlibakken, Lake Tahoe, California, February 26–29, Alan Liss, New York, **1988**.

5 Nerem RM, Cellular engineering, *Ann. Biomed. Eng.* 19, 529–545, **1991**.

6 Langer R, Vacanti JP, Tissue engineering. *Science* 260, 920–926, **1993**.

7 Vacanti JP, Langer R, Tissue engineering: the design and fabrication of living replacement devices for surgical reconstruction and transplantation. *Lancet* 354 (Suppl 1), 32–34, **1999**.

8 Fuchs JR, Nasseri BA, Vacanti JP. Tissue engineering: A 21st century solution to surgical reconstruction. *Ann. Thorac. Surg.* 72, 577–591, **2001**.

9 Laurencin CT, Amborsio AMA, Borden MD, Cooper JA. Tissue engineering: orthopedic application. *Ann. Rev. Biomed. Eng.* 1, 19–46, **1999**.

10 Sipe JD. Tissue engineering and reparative medicine. *Ann. New York Acad. Sci.* 961, 1–9, **2002**.

11 Weaver VM, Petersen OW, Wang F, Larabell CA, Briand P, Damsky C, Bissell MJ. Reversion of the malignant phenotype of human breast cells in three-dimensional culture and in vivo by integrin blocking antibodies. *J. Cell Biol.* 137, 231–245, **1997**.

12 Cukierman E, Pankov R, Stevens DR, Yamada KM. Taking cell-matrix adhesions to third dimensions. *Science* 294, 1708–1712, **2001**.

13 Vacanti JP, Morse MA, Saltzman WM, Domb AJ, Perezatyde A, Langer R. Selective cell transplantation using bioabsorbable artificial polymers as matrices. *J. Pediar. Surg.* 23, 3–9, **1988**.

14 Langer R, Tirrell DA, Designing materials for biology and medicine. *Nature* 428, 487–492, **2004**.

15 Rosso F, Mario G, Giordano A, Barbarisi M, Parmeggiani D, Barbarusu A. Smart materials as scaffolds for tissue engineering. *J. Cell Physiol.* 203, 465–470, **2005**.

16 Mallapragada S, Narasimhan B (Eds.), *Handbook of Biodegradable Polymeric Materials and their Applications*. American Scientific Publishers, North Lewis Way, **2006**.

17 Hollister SJ. Porous scaffold design for tissue engineering. *Nat. Mater.* 4, 518–524, **2005**.

18 Agarwal CM, Ray RB. Biodegradable polymeric scaffolds for musculoskeletal regeneration. *J. Biomed. Mater. Res.* 55, 141–150, **1988**.

19 Lu L, Mikos AG. The importance of new processing techniques in tissue engineering. *MRS Bull.* 11, 28, **1996**.

20 Thomson RC, Yaszemski MJ, Mikos AG. Polymer scaffold processing. In: Lanza RP, Langer R, Chick WL (Eds.), *Principles of Tissue Engineering*. R.G. Landes Co., Austin, TX, p. 263, **1997**.

21 Widmer MS, Mikos AG. Fabrication of biodegradable polymer scaffolds for tissue engineering. In: Patrick Jr CW, Mikos AG, McIntire LV (Eds.), *Frontiers in Tissue Engineering*. Elsevier Science, New York, p. 107, **1998**.

22 Hutmacher DW, Zein I, Teoh SH, Ng KW, Schantz JT, Leahy JC. Design and fabrication of a 3D scaffold for tissue engineering bone. In: Agarwal CM, Parr JE, Lin ST (Eds.), *Synthetic Bioabsorbable Polymers for Implants*, STP 1396. American Society for Testing and Materials, West Conshohocken, PA, p. 152, **2000**.

23 Hutmacher DW, Sittinger M, Risbud MV. Scaffold-based tissue engineering: rationale for computer aided design and solid free form fabrication systems. *Trends Biotechnol.* 22, 354–362, **2004**.

24 Mikos AG, Thorsen AJ, Czerwonka LA, Bao Y, Langer R, Winslow DN, Vacanti JP. Preparation and characterization of poly(L-lactic acid) foams. *Polymer* 35, 1068–1077, **1994**.

25 Ma, PX, Langer R. Fabrication of biodegradable polymer foams for cell transplantation and tissue

engineering. In: Morgan J, Yarmush M (Eds.), *Tissue Engineering Methods and Protocols*, Humana Press, NJ, p. 47, **1999**.
26 Lu L, Peter SJ, Lyman MD, Lai H, Leite SM, Tamada JA, Vacanti JP, Langer R, Mikos AJ. *In vitro* degradation of porous poly(L-lactic acid) foams. *Biomaterials* 21, 1595–1605, **2000**.
27 Borden MD, Khan Y, Attawia M, Laurencin CT. Tissue engineered microsphere-based matrices for bone repair: Design, evaluation, and optimization. *Biomaterials* 23, 551–9, **2002**.
28 Borden M, Attawia M, Laurencin CT. The sintered microsphere matrix for bone tissue engineering: In vitro osteoconductivity studies. *J. Biomed. Mater. Res.* 61, 421–429, **2002**.
29 Borden MD, El-Amin SF, Attawia M, Laurencin CT. Structural and human cellular assessment of a novel microsphere based tissue engineered scaffold for bone repair. *Biomaterials*, 24, 597–609, **2003**.
30 Borden MD, Attawia M, Khan Y, El-Amin SF, Laurencin CT. Tissue-engineered bone formation *in vivo* using a novel sintered polymeric microsphere matrix. *J. Bone Joint Surg. (B)*. 86-B, 1200–1208, **2004**.
31 Yang SF, Leong KF, Du ZH, Chua CK. The design of scaffolds for use in tissue engineering: part 1 – Traditional factors. *Tissue Eng.* 7, 679–689, **2001**.
32 Leong KF, Cheah CM, Chua CK. Solid freeform fabrication of three-dimensional scaffolds for engineering replacement tissues and organs, *Biomaterials* 24, 2363–2378, **2003**.
33 Cooke MN, Fisher JP, Dean D, Rimnac C, Mikos AG. Use of stereolithography to manufacture critical-sized 3D biodegradable scaffolds for bone ingrowth, *J. Biomed. Mater. Res.* 64B, 65–69, **2003**.
34 Yu T, Chiellini F, Schmaljohann D, Solaro R, Ober CK. Microfabrication of hydrogels as polymer scaffolds for tissue engineering applications. *Polym. Prepr.* 41, 1699–1700, **2000**.
35 Gariepy E, Leroux J. In situ forming hydrogels – Review of temperature sensitive systems. *Eur. J. Pharm. Biopharm.* 58, 409–426, **2004**.
36 Gil ES, Hudson SM. Stimuli-responsive polymers and their bioconjugates. *Progr. Polym. Sci.* 29, 1173–1222, **2004**.
37 Kim TM, Sharma B, Williams CG, Ruffner MA, Malik A, McFarland EG, Elisseeff JH. Experimental model for cartilage tissue engineering to regenerate the zonal organization of articular cartilage. *Osteoarthritis Cartilage* 11, 653–664, **2003**.
38 Varghese D, Deshpande M, Xu T, Kesari P, Ohri S, Boland T. Advances in tissue engineering: cell printing. *J. Thor. Card. Surg.* 129, 470–472, **2005**.
39 Boland T, Mironov V, Gutowska A, Roth EA, Markwald RR. Cell and organ printing 2: Fusion of cell aggregates in three-dimensional gels. *Anat. Rec.* 272A, 497–502, **2003**.
40 Neagu A, Forgac G. Fusion of cell aggregates: a mathematical model. In: Vossoughi J (Ed.), *Biomedical Engineering. Recent Development*, Medical and Engineering Publishers, Inc., Washington DC, USA, pp. 241–242, **2002**.
41 Mironov V, Boland T, Trusk T, Forgacs G, Markwald RR. Organ printing: Computer-aided jet-based 3D tissue engineering. *Trends Biotechnol.* 21, 157–161, **2003**.
42 Jakab K, Neagu A, Mironov V, Markwald RR, Forgacs G. Engineering biological structures of prescribed shape using self-assembling multicellular systems, *Proc. Natl. Acad. Sci. U.S.A.* 10, 2864–2869, **2004**.
43 Shieh S, Terada S, Vacanti JP. Tissue engineering auricular regeneration: *In vitro* and *in vivo* studies. *Biomaterials*. 25, 1545–1557, **2004**.
44 Raspanti M, Protasoni M, Manelli A, Guizzardi S, Mantovani V, Sala A. The extracellular matrix of the human aortic wall: Ultrastructural observations by FEG-SEM and by tapping-mode AFM. *Micron*. 37, 81–86, **2006**.
45 Griffith LG. Emerging design

principles in biomaterials and scaffolds in tissue engineering. *Ann. New York Acad. Sci.* 961, 83–95, **2002**.

46 Saltzmann WM, Olbricht WL. Building drug delivery into tissue engineering. *Nat. Rev. Drug Discov.* 1, 177–186, **2002**.

47 Tirrell M, Kokkoli E, Biesalski M. The role of surface science in bioengineered materials. *Surf. Sci.* 500, 61–83, **2002**.

48 Bosman FT, Stamenkovic I. Functional structure and composition of the extracellular matrix. *J. Pathol.* 200, 432–428, **2003**.

49 Olsen BR. Matrix molecules and their ligands. In: Lanza RP, Langer R, Chick WL (Eds.), *Principles of Tissue Engineering*, 1st edition, Academic Press, New York, pp. 47–65, **1997**.

50 Boudreau N, Myers C, Bissell MJ. From laminin to lamin: regulation of tissue-specific gene expression by the ECM. *Trends Cell Biol.* 5, 1–4, **1995**.

51 Provenzane PP, Vanderby R. Collagen fibril morphology and organization: Implications for force transmission in ligament and tendon. *Matrix Biol.* 25, 71–84, **2006**.

52 Fantner GE, Rabinovych O, Schitter G, Thurner P, Kindt JH, Finch MM, Weaver JC, Golde LS, Morse DE, Lipman EA, Rangelow IW, Hansma PK. Hierarchical interconnections in the nano-composite material bone: Fibrillar cross-links resist fracture on several length scales. *Composites Sci. Technol.* 66, 1205–1211, **2006**.

53 Gelse K, Poschl E, Aigner T. Collagen Structure, function and biosynthesis. *Adv. Drug Deliv. Rev.* 55, 1531–1546, **2003**.

54 Curtis A, Wilkinson C. Nano-techniques and approaches in biotechnology. *Trends Biotechnol.* 19, 97–101, **2001**.

55 Lutolf MP, Hubbell JA. Synthetic biomaterials as instructive extra-cellular microenvironments for mor-phogenesis in tissue engineering. *Nat. Biotechnol.* 23, 47–55, **2005**.

56 Adams JC, Watt FM. Regulation of development and differentiation by the extracellular matrix. *Development* 117, 1183–1198, **1993**.

57 Xiong J, Stehle T, Diefenbach B, Zhang R, Dunker R, Scott DL, Joachimiak A, Goodman SL, Arnaouti MA, Crystal structure of the extracellular segment of integrin $\alpha V\beta 3$. *Science* 294, 339–345, **2001**.

58 Garcia AJ. Get a grip. Integrins in cell–biomaterial interactions *Biomaterials* 26, 7525–7529, **2005**.

59 Bershadsky AD, Ballestrem C, Carramusa L, Zilberman Y, Gilquin B, Khochbin S, Alexandrova AY, Verkhovsky AB, Shemesh T, Kozlov MM. Assembly and mechanosensory function of focal adhesions: experiments and models *Eur. J. Cell Biol.* 85, 165–173, **2006**.

60 Ross RS. Molecular and mechanical synergy: Cross-talk between integrins and growth factor receptors. *Cardiovasc. Res.* 63, 381– 390, **2004**.

61 Adams JC, Cell matrix contact structure. *Cell Mol. Life Sci.* 58, 371–392, **2001**.

62 He L, Dexter AF, Middleberg APJ. Biomolecular engineering at interfaces. *Chem. Eng. Sci.* 61, 989–1003, **2006**.

63 Li JM, Menconi MJ, Wheeler HB, Rohrer MJ, Kiassen VA, Ansell JE, Appel MC. Precoating expanded polytetrafluoroethylene grafts alters production of endothelial cell-derived thrombomodulators. *J. Vasc. Surg.* 15, 1010–1017, **1992**.

64 Kaehler J, Zilla P, Fasol R, Deutsch M, Kadletz M. Precoating substrate and surface configuration determine adherence and spreading of seeded endothelial cells on polytetrafluoroethylene grafts. *J. Vasc. Surg.* 9, 535–41, **1989**.

65 Seeger JM, Klingman N. Improved endothelial cell seeding with cultured cells and fibronectin-coated grafts. *J. Surg. Res.* 38, 641–7, **1985**.

66 Pierschbacher MD, Ruoslahti E. Cell attachment activity of fibronectin can be duplicated by small synthetic fragments of the molecule. *Nature* 309, 30–33, **1984**.

67 Ruoslahti E, Pierschbacher MD. New perspectives in cell adhesion:

RGD and integrins. *Science* 238, 491–497, **1987**.

68 Ruoslahti E. RGD and other recognition sequences for integrins. *Annu. Rev. Cell Dev. Biol.* 12, 697–715, **1996**.

69 Ruoslahti E. The RGD story. A personal account. *Matrix Biol.* 22, 459–465, **2003**.

70 Hynes RO. Integrins – Versatility, modulation, and signaling in cell-adhesion. *Cell* 69, 11–25, **1992**.

71 Xiong JP, Stehle T, Zhang R, Joachimiak A, Frech M, Goodman SL, Arnaout MA. Crystal structure of the extracellular segment of integrin avb3 in complex with an Arg–Gly Asp ligand. *Science* 296, 151–155, **2002**.

72 Xiong J, Stehle T, Goodman SL, Arnaouti MA. A novel adaptation of the integrin PSI domain revealed from its crystal structure. *J. Biol. Chem.* 279, 40 252–40 254, **2004**.

73 Ito Y, Kajihara M, Imanishi Y. Materials for enhancing cell adhesion by immobilization of cell-adhesive peptide. *J. Biomed. Mater. Res.* 25, 1325–37, **1991**.

74 Neff JA, Caldwell KD, Tresco PA. A novel method for surface modification to promote cell attachment to hydrophobic substrates. *J. Biomed. Mater. Res.* 40, 511–519, **1998**.

75 Hersel U, Dahmen C, Kessler H. RGD modified polymers: Biomaterials for simulated cell adhesion and beyond. *Biomaterials* 24, 4385–4415, **2003**.

76 Pelham Jr RJ, Wang YL. Cell locomotion and focal adhesions are regulated by the mechanical properties of the substrate. *Biol. Bull.* 194, 348–50, **1998**.

77 Castel S, Pagan R, Mitjans F, Piulats J, Goodman S, Jonczyk A, Huber F, Vilaro S, Reina M. RGD peptides and monoclonal antibodies, antagonists of avb3-integrin, enter the cells by independent endocytic pathways. *Lab. Invest.* 81, 1615–1626, **2001**.

78 Yang XB, Roach HI, Clarke NM, Howdle SM, Quirk R, Shakesheff KM, Oreffo RO. Human osteoprogenitor growth and differentiation on synthetic biodegradable structures after surface modification. *Bone* 29, 523–531, **2001**.

79 Neff JA, Tresco PA, Caldwell KD. Surface modification for controlled studies of cell–ligand interactions. *Biomaterials* 20, 2377–2393, **1999**.

80 Hirano Y, Okuno M, Hayashi T, Goto K, Nakajima A. Cell attachment activities of surface immobilized oligopeptides RGD, RGDS, RGDV, RGDT, and YIGSR toward five cell lines. *J. Biomater. Sci. Polym. Ed.* 4, 235–243, **1993**.

81 Cook AD, Hrkach JS, Gao NN, Johnson IM, Pajvani UB, Cannizzaro SM, Langer R. Characterization and development of RGD-peptide-modified poly(lactic acid-co-lysine) as an interactive, resorbable biomaterial. *J. Biomed. Mater. Res.* 35, 513–523, **1997**.

82 Breuers W, Klee D, Hocker H, Mittermayer C. Immobilization of a fibronectin fragment at the surface of a polyetherurethane film. *J. Mater. Sci. Mater. Med.* 2, 106–109, **1991**.

83 Tong YW, Shoichet MS. Peptide surface modification of poly(tetrafluoro-ethylene-co-hexafluoropropylene) enhances its interaction with central nervous system neurons. *J. Biomed. Mater. Res.* 42, 85–95, **1998**.

84 Porte-Durrieu MC, Labrugere C, Villars F, Lefebvre F, Dutoya S, Guette A, Bordenave L, Baquey C. Development of RGD peptides grafted onto silica surfaces: XPS characterization and human endothelial cell interactions. *J. Biomed. Mater. Res.* 46, 368–375, **1999**.

85 Marchand-Brynaert J. Surface modifications and reactivity assays of polymer films and membranes by selective wet chemistry. *Recent Res. Polym. Sci.* 2, 335–361, **1998**.

86 Carlisle ES, Mariappan MR, Nelson KD, Thomes BE, Timmons RB, Constantinescu A, Eberhart RC, Bankey PE. Enhancing hepatocyte adhesion by pulsed plasma deposition and polyethylene glycol coupling. *Tissue Eng.* 6, 45–52, **2000**.

87 Tam JP, Yu Q, Miao Z. Orthogonal ligation strategies for peptide and protein. *Biopolymers* 51, 311–332, **1999**.

88 Ivanov B, Grzesik W, Robey FA. Synthesis and use of a new bromoacetyl-derivatized heterotrifunctional amino acid for conjugation of cyclic RGD-containing peptides derived from human bone sialoprotein. *Bioconj. Chem.* 6, 269–277, **1995**.

89 Houseman BT, Gawalt ES, Mrksich M. Maleimide functionalized self-assembled monolayers for the preparation of peptide and carbohydrate biochips. *Langmuir* 19, 1522–1531, **2003**.

90 Herbert CB, McLernon TL, Hypolite CL, Adams DN, Pikus L, Huang CC, Fields GB, Letourneau PC, Distefano MD, Hu WS. Micropatterning gradients and controlling surface densities of photoactivatable biomolecules on self-assembled monolayers of oligo(ethylene glycol) alkanethiolates. *Chem. Biol.* 4, 731–737, **1997**.

91 Lin YS, Wang SS, Chung TW, Wang YH, Chiou SH, Hsu JJ, Chou NK, Hsieh KH, Chu SH. Growth of endothelial cells on different concentrations of Gly Arg-Gly Asp photochemically grafted in poly-ethylene glycol modified polyurethane. *Artif. Organs* 25, 617–621, **2001**.

92 Sugawara T, Matsuda T. Photochemical surface derivatization of a peptide containing Arg–Gly Asp (RGD). *J. Biomed. Mater. Res.* 29, 1047–1052, **1995**.

93 Reyes CD, Garcia AJ. Engineering integrin-specific surfaces with a triple helical collagen mimetic peptide. *J. Biomed. Mater. Res. Part A* 65, 511–523, **2003**.

94 Kantlehner M, Schaffner P, Finsinger D, Meyer J, Jonczyk A, Diefenbach B, Nies B, Holzemann G, Goodman SL, Kessler H. Surface coating with cyclic RGD peptides stimulates osteoblast adhesion and proliferation as well as bone formation. *Chem-BioChem* 1, 107–114, **2000**.

95 Delforge D, Gillon B, Art M, Dewelle J, Raes M, Remacle J. Design of a synthetic adhesion protein by grafting RGD tailed cyclic peptides on bovine serum albumin. *Lett. Pept Sci.* 5, 87–91, **1998**.

96 Kao WJ, Hubbell JA, Anderson JM. Protein-mediated macrophage adhesion and activation on biomaterials: A model for modulating cell behavior. *J. Mater. Sci. Mater. Med.* 10, 601–605, **1999**.

97 Massia SP, Stark J. Immobilized RGD peptides on surface grafted dextran promotes biospecific cell attachment. *J. Biomed. Mater. Res.* 56, 390–9, **2001**.

98 Massia SP, Hubbell JA. An RGD spacing of 440 nm is sufficient for integrin avb3-mediated fibroblast spreading and 140 nm for focal contact fiber formation. *J. Cell. Biol.* 114, 1089–1100, **1991**.

99 Elbert DL, Hubbell JA. Conjugate addition reactions combined with free-radical cross-linking for the design of materials for tissue engineering. *Biomacromolecules* 2, 430–441, **2001**.

100 Irvine DJ, Hue KA, Mayes AM, Griffith LG. Simulations of cell-surface integrin binding to nanoscale-clustered adhesion ligands. *Biophys. J.* 82, 120–132, **2002**.

101 Maheshwari G, Brown G, Lauffenburger DA, Wells A, Griffith LG. Cell adhesion and motility depend on nanoscale RGD clustering. *J. Cell Sci.* 113, 1677–1686, **2000**.

102 Irvine DJ, Ruzette A-VG, Mayes AM, Griffith LG. Nanoscale clustering of RGD peptides at surfaces using comb polymers – 2. Surface segregation of comb polymers in polylactide. *Biomacromolecules* 2, 545–56, **2001**.

103 Interagency Working Groups on Nanoscience, and Technology, National Nanotechnolgy Initiative: Leading to the Next Industrial Revolution. Washington D.C., Committee on Technology, National Science and Technology Council, **2000**.

104 Alivisatos AP. Semiconductor

clustors, nanocrystals, and quantum dots. *Science* 271, 933–937, **1996**.

105 Simon A, Durrieu M. Strategies and results of atomic force microscopy in the study of cellular adhesion. *Micron* 37, 1–13, **2006**.

106 Woodcock SE, Johnson WC, Chen Z. Collagen adsorption and structure on polymer surfaces observed by atomic force microscopy. *J. Colloid Interface Sci.* 292, 99–107, **2005**.

107 Curtis AS, Casey B, Gallagher JO, Pasqui D, Wood MA, Wilkinson CD. Substratum nanotopography and the adhesion of biological cells. Are symmetry or regularity of nanotopography important? *Biophys. Chem.* 94, 275–283, **2001**.

108 Dalby MJ, Yarwood SJ, Riehle MO, Joshstone HJH, Affrossman S, Curtis ASG. Increasing fibroblast response to materials using nanotopography: morphological and genetic measurements of cells response to 13 mm-high polymer demixed islands. *Exp. Cell Res.* 276, 1–9, **2002**.

109 Dalby MJ, Childs S, Riehle MO, Johnstone HJH, Affrossman S, Curtis ASG. Fibroblast reaction to island topography; changes in cytoskeleton and morphology with time. *Biomaterials* 24, 927–935, **2003**.

110 Dalby MJ, Giannaras D, Riehle MO, Gadegaard N, Affrossman S, Curtis ASG. Rapid fibroblast adhesion to 27 nm high polymer demixed nanotopography. *Biomaterials* 25, 77–83, **2004**.

111 Dalby MJ, McCloy D, Robertson M, Wilkinson CDW, Oreffo ROC. Osteoprogenitor response to defined topographies with nanoscale depths. *Biomaterials* 27, 1306–1315, **2006**.

112 Nair LS, Bhattacharyya S, Laurencin CT. Development of novel tissue engineering scaffolds via electrospinning. *Expert Opin. Biol. Ther.* 4, 1–10, **2004**.

113 Chronakis IS. Novel nanocomposites and nonoceramics based on polymer nanofibers using electrospinning process – A review. *J. Mater. Process Tec.* 167, 283–293, **2005**.

114 Smith LA, Ma PX, Nanofibrous scaffolds for tissue engineering. *Collids Surf. B: Biointerfaces* 39, 125–131, **2004**.

115 Martin CR. Membrane based synthesis of nanomaterials. *Chem. Mater.* 8, 1739–1746, **1996**.

116 Jayaraman K, Kotaki M, Zhang Y, Mo X, Ramakrishna S. Recent advances in polymer nanofibers. *J. Nanosci. Nanotechnol.* 4, 52–65, **2004**.

117 Taylor GI. *Proc. Royal Soc. London* A313, 453, **1969**.

118 Reneker JD, Electrospinning process and applications of electrospun fibers. *J. Electrostatics* 35, 151, **1995**.

119 Reneker DH, Yarin AL, Fong H, Koombhongse S, *J. Appl. Phys.* 87, 4531, **2000**.

120 Reneker DH, Yarin A, Evans EA, Kataphinan W, Rangkupan R, Liu W. *Electrospinning and Nanofibers*, Book of Abstracts. In: New Frontiers in Fiber Science, Spring Meeting 2001. Available from: http://www.tx.ncsu.edu/jtatm/volume1specialissue/presentations/pres_part1.doc.

121 Yarin AL, Reneker DH. Taylor cone and jetting from liquid droplets in electrospinning of nanofibers. *J. Appl. Phys.* 90, 4836–4846, **2001**.

122 Shin MY, Hohman MM, Brenner M, Ruteldge GC. Experimental characterization of electrospinning: The electrically forced jet and instabilities. *Polymer* 42, 9955–9967, **2001**.

123 Nair LS, Bhattacharyya S, Bender JD, Greish YE, Brown PW, Allcock HR, Laurencin CT. Fabrication and optimization of methylphenoxy substituted polyphosphazene nanofibers for biomedical applications. *Biomacromolecules*, 5, 2212–2220, **2004**.

124 Frenot A, Chronakis IS. Polymer nanofibers assembled by electrospinning. *Curr. Opin. Colloid Inter. Sci.* 8, 64–75, **2003**.

125 Reneker DH, Chun I. Nanometric diameter fibers of polymer produced by electrospinning. *Nanotechnology*, 7, 216–223, **1996**.

126 Huang Z, Zang YZ, Kotaki M,

Ramakrishana S. A review on polymer nanofibers by electrospinning and their applications in nanocomposites. *Composites Sci. Technol.* 63, 2223–2253, **2003**.

127 Morota K, Matsumoto H, Mizukoshi T, Konosu Y, Minagawa M, Tanioka A, Ya, agata Y, Inoue K. Poly(ethylene oxide) thin films produced by electrospray deposition: Morphology control and additive effects of alcohols on nanostructure. *J. Colloid Interface Sci.* 279, 484–492, **2004**.

128 Katti DS, Robinson KW, Ko FK, Laurenicn CT. Bioresorbable nanofiber-based systems for wound healing and drug delivery: Optimization of fabrication parameters. *J. Biomed. Mater. Res. Part B, Appl. Biomater.* 70, 286–296, **2004**.

129 Deitzel JM, Kleinmeyer D, Hirvanen JK, Tan NCB. Controlled deposition of electrospun poly(ethylene oxide) fibers. *Polymer* 42, 8163–8170, **2001**.

130 Demir MM, Yilgor I, Yilgor E, Erman B. Electrospinning of polyurethane fibers. *Polymer* 43, 3303–3309, **2002**.

131 Deitzel JM, Kleinmeyer J, Harris D, Tan NCB. The effect of processing variables on the morphology of electrospun nanofibers and textiles. *Polymer* 42, 261–272, **2001**.

132 Zong X, Kim K, Fang D, Ran S, Hsiao BS, Chu B. Structure and process relationship of electrospun bioabsorbable nanofiber membranes. *Polymer* 43, 4403–4412, **2002**.

133 Koombhongse S, Liu W, Reneker DH. Flat ribbons and other shapes by electrospinning. *J. Polym. Sci., Polym. Phys. Ed.* 39, 2598–2606, **2001**.

134 Bognitzki M, Czado W, Frese T, Schaper A, Hellweg M, Steinhart M, Greiner A, Wendorff JH. *Adv. Mater.* 13, 70, **2001**.

135 Megelski S, Stephens JS, Chase DB, Rabolt JF. Micro- and nanostructured surface morphology on electrospun polymer fibers. *Macromolecules* 35, 8456–8466, **2002**.

136 Casper CL, Stephens JS, Tassi NG, Chase DB, Rabolt JF. Controlling surface morphology of electrospun polystyrene fibers: Effect of humidity and molecular weight in the electrospinning process. *Macromolecules* 37, 573–578, **2004**.

137 Matthews JA, Wnek GE, Simpson DG, Bowlin GL. Electrospinning of collagen nanofibers. *Biomacromolecules* 3, 232–238, **2002**.

138 Bornat A. Production of electrostatically spun products. *US Patent 4689186*, **1987**.

139 Theron A, Zussman E, Yarin AL. Electrostatic field-assisted alignment of electrospun nanofibres. *Nanotechnology* 12, 384–390, **2001**.

140 Xu CY, Inai R, Kotaki M, Ramakrishna S. Aligned biodegradable nanofibrous structure: A potential scaffold for blood vessel engineering. *Biomaterials* 25, 877–886, **2004**.

141 Ding B, Kim HY, Kim CK, Khil MS, Park SJ. *Nanotechnology* 14, 532–537, **2003**.

142 Kenawy ER, Bowlin GL, Mansfieled K, Laman J, Simpson DG, Sander EH, Wnek GE. *J. Controlled Release* 81, 57–64, **2002**.

143 Sun ZC, Zussman E, Yarin AL, Wendorff JH, Greiner A. *Adv. Mater.* 15, 1929, **2003**.

144 Ding B, Kimura E, Sato T, Fujita S, Shiratori S. Fabrication of blend biodegradable nanofibrous nonwoven mats via multijet electrospinning. *Polymer* 45, 1895–1902, **2004**.

145 Gupta P, Wilkes GL. Some investigations on the fiber formation by utilizing a side-by-side bicomponent electrospinning approach. *Polymer* 44, 6353–6359, **2003**.

146 Stankus JJ, Guan J, Wagner WR. Fabrication of biodegradable elastomeric scaffolds with sub-micron morphologies. *J. Biomed. Mater. Res.* 70, 603–614, **2004**.

147 Hamdan AL, Daniel SJ, Laura HM, Reneker D. Preservation of enzymes in electrospun nanofibers. Technical Papers – American Chemical Society, Rubber Division, Spring Technical Meeting, 163rd, San Francisco, 28–30 April 2003.

148 Jiang H, Hu Y, Li Y, Zhao P, Zhu K, Chen W. A facile technique to prepare biodegradable coaxial electrospun nanofibers for controlled release of bioactive agents. *J. Controlled Release* 108, 237–243, **2005**.

149 Li WJ, Laurencin CT, Caterson EJ, Tuan RS, Ko FK. Electrospun nanofibrous structure: A novel scaffold for tissue engineering. *J. Biomed. Mater. Res.* 60, 613–621, **2002**.

150 He W, Ma ZW, Yong T, Teo WE, Ramakrishna S. Fabrication of collagen-coated biodegradable polymer nanfiber mesh and its potential for endothelial cells growth. *Biomaterials* 26, 7606–7615, **2005**.

151 Kwon K, Kodoaki S, Matsuda T. Electrospun nano- to microfiber fabrics made of biodegradable copolyesters: Structural characteristics, mechanical properties and cell adhesion potential. *Biomaterials* 26, 3929–3939, **2005**.

152 Lee SH, Ku BC, Wang X, Samuelson LA, Kumar J. Design, synthesis and electrospinning of a novel fluorescent polymer for optical sensor applications. *Mater. Res. Soc. Symp. Proc.* 708, 403–408, **2002**.

153 Lee CH, Shin HJ, Cho IH, Kang YM, Kim IA, Park KD, Shin JW. Nanofiber alignment and direction of mechanical strain affect the ECM production of human ACL fibroblast. *Biomaterials* 26, 1261–1270, **2005**.

154 Ma PX, Zhang R. Synthetic nano-scale fibrous. *J. Biomed. Mater. Res.* 46, 60–72, **1999**.

155 Wei G, Ma PX. Structure and properties of nano-hydroxyapatite/ polymer composite scaffolds for bone tissue engineering *Biomaterials* 25, 4749–4757, **2004**.

156 Zhang R, Ma PX. Synthetic nano-fibrillar extracellular matrices with predesigned macroporous architectures. *J. Biomed. Mater. Res.* 52, 430–438, **2000**.

157 Whitesides GA, Mathias JP, Seto CT. *Science* 254, 1312, **1991**.

158 Zhang S. Building from bottom-up. *Mater. Today* 6, 20–27, **2003**.

159 Zhang S, Holmes T, Lockshin L, Rich A. Spontaneous assembly of a self-complementary oligopeptide to form a stable macroscopic membrane. *Proc. Natl. Acad. Sci. U.S.A.* 90, 3334–3338, **1993**.

160 Zhang S. Molecular self-assembly. In: Buschon KH et al. (Eds.), *The Encyclopdia of Materials Science and Technology*, Elsevier Science, Oxford, pp. 5822–5829, **2001**.

161 Zhao Z, Zhang S. Fabrication of molecular materials using peptide construction motifs. *Trends Biotechnol.* 22, 470–476, **2004**.

162 Hartgerink JD, Beniash E, Stupp SI. Self assembly and mineralization of peptide amphiphile nanofibers. *Science* 294, 1684–1688, **2001**.

163 Niece KL, Hartgerink JD, Donnors JJM, Stupp SI. Self assembly combining two bioactive peptide-amphiphile molecules into nanofibers by electrostatic attraction. *J. Am. Chem. Soc.* 125, 7146–7147, **2003**.

164 Petka WA, Harden JL, McGrath KP, Wirtz D, Tirrell DA. Reversible hydrogels from self-assembling artificial proteins. *Science* 281, 389–392, **1998**.

165 Nowak AP, Breedveld V, Pakstis L, Ozbas B, Pine DJ, Pochan D, Deming TJ. Rapidly recovering hydrogel scaffolds from self assembling diblock copolypeptide amphiphiles. *Nature* 417, 424–428, **2002**.

166 Schindler M, Ahmed I, Kamal J, Nur-E-Kamal A, Grafe TH, Chung HY, Meiners S. A synthetic nanofibrillar matrix to promote *in vivo*-like organization and morphogenesis for cell in culture. *Biomaterials* 26, 5624–5631, **2005**.

167 Wozniak MA, Desai R, Solski PA, Der CJ, Keely PJ, ROCK generated contractility regulates breast epithelial cell differentiationin response to the physical properties of a three-dimensional collagen matrix. *J. Cell. Biol.* 163, 583–595, **2003**.

168 Silva GA, Czeisler C, Niece KL, Beniash E, Harrington DA, Kessler JA, Stupp SI. Selective differentiation of neural progenitor cells by high-

epitope density nanofibers. *Science* 303, 1352–1355, **2004**.

169 Li W, Tuli R, Huang X, Laquerriere P, Tuan RS. Multilineage differentiation of human mesenchymal stem cells in a three-dimensional nanofibrous scaffold. *Biomaterials* 26, 5158–5166, **2005**.

170 Yang F, Murugan R, Ramakrishna S, Wang X, Ma YX, Wang S. Fabrication of nano-structured porous PLLA scaffold intended for nerve tissue engineering. *Biomaterials* 25, 1891–1900, **2004**.

171 Yang F, Murugan R, Wang S, Ramakrishana S. Electrospinning of nano/micro scale poly(L-lactic acid) aligned fibers and their potential in neural tissue engineering. *Biomaterials* 26, 2603–2610, **2005**.

172 Mo ZM, Xu CY, Kotaki M, Ramakrishna S. Electrospin (P(LLA-CL) nanofiber: A biomimetic extracellular matrix for smooth muscle cell and endothelial cell proliferation. *Biomaterials* 25, 1883–1890, **2004**.

173 Venugopal J, Ma LL, Yong T. Ramakrishna S. In vitro study of smooth muscle cells on polycaprolactorn and collagen nanofibrous matrices. *Cell Biol. Int.* 29, 861–867, **2005**.

174 Ma Z, Kotaki M, Yong T, He W, Ramakrishnan S. Surface engineering of electrospun polyethylene terephthalate (PET) nanofibers towards development of a new material for blood vessel engineering. *Biomaterials* 26, 2527–2536, **2005**.

175 Genove E, Shen C, Zhang S, Semino CE. The effect of functionalized self-assembling peptide scaffolds on human aortic endothelial cell function. *Biomaterials* 26, 3341–3351, **2005**.

176 Shin M, Ishii O, Sueda T, Vacanti JP. Contractile cardiac grafts using a novel nanofibrous mesh. *Biomaterials* 25, 3717–3723, **2004**.

177 Ishii O, Shin M, Sueda T, Vacanti JP. In vitro tissue engineering of a cardiac graft using a degradable scaffold with an extracellular matrix-like topography. *J. Thor. Cardiovasc. Surg.* 130, 1358–1363, **2005**.

178 Yoshimoto H, Shin YM, Terai H, Vacanti JP. A biodegradable nanofiber scaffold by electrospinning and its potential for bone tissue engineering. *Biomaterials*, 24, 2077–2082, **2003**.

179 Li W, Tuli R, Huang X, Okafor C, Derfoul A, Danielson KG, Hall DJ, Tuan RS. A three-dimensional nanofibrous scaffold for cartilage tissue engineering using human mesenchymal stem cells. *Biomaterials* 26, 599–609, **2005**.

180 Kisiday J, Jin M, Kurz B, Hung H, Semino C, Zhang S, Grodzinsky AJ. Self assembling peptide hydrogel fosters chondrocyte extracellular matrix production and cell division: implications for cartilage tissue repair. *Proc. Natl. Acad. Sci. U.S.A.* 99, 9996–10 001, **2002**.